Check for updates

Comparative soft-tissue preservation in Holocene-age capelin concretions

Angel Mojarro[1*], Xingqian Cui[1#], Xiaowen Zhang[1#], Adam Jost[1], Kristin Bergmann[1], Jakob Vinther[2], and Roger E. Summons[1]

[1]Department of Earth, Atmospheric and Planetary Sciences, Massachusetts Institute of Technology, Cambridge, Massachusetts, United States.
[2]School of Biological Sciences, University of Bristol, Bristol, United Kingdom.

*Address correspondence to:
Angel Mojarro
Massachusetts Institute of Technology
77 Massachusetts Ave, Room E25-647
Cambridge, MA, 02139
E-mail: mojarro@mit.edu

[#]Current address: School of Oceanography, Shanghai Jiao Tong University, Shanghai, China.

Acknowledgements

This work was supported by the MIT Dean of Science Fellowship. Laboratory work at MIT was supported by the Simons Foundation, Collaboration on the Origins of Life (SCOL) through an award (290361FY18) to RES. We would like to thank Michelle Coyne at the Geological Survey of Canada, Professor Derek Briggs, Ben Uveges, and Lise Lawaetz.

This is the author manuscript accepted for publication and has undergone full peer review but has not been through the copyediting, typesetting, pagination and proofreading process, which may lead to differences between this version and the Version of Record. Please cite this article as doi: 10.1111/GBI.12480

This article is protected by copyright. All rights reserved

Comparative soft-tissue preservation in Holocene-age capelin concretions

Angel Mojarro[1*], Xingqian Cui[1#], Xiaowen Zhang[1#], Adam B. Jost[1], Kristin D. Bergmann[1], Jakob Vinther[2], and Roger E. Summons[1]

[1]Department of Earth, Atmospheric and Planetary Sciences, Massachusetts Institute of Technology, Cambridge, Massachusetts, United States.
[2]School of Biological Sciences, University of Bristol, Bristol, United Kingdom.

*Address correspondence to:
Angel Mojarro
Massachusetts Institute of Technology
77 Massachusetts Ave, Room E25-647
Cambridge, MA, 02139
E-mail: mojarro@mit.edu

[#]Current address: School of Oceanography, Shanghai Jiao Tong University, Shanghai, China.

Acknowledgements

This work was supported by the MIT Dean of Science Fellowship. Laboratory work at MIT was supported by the Simons Foundation, Collaboration on the Origins of Life (SCOL) through an award (290361FY18) to RES. We would like to thank Michelle Coyne at the Geological Survey of Canada, Professor Derek Briggs, Ben Uveges, and Lise Lawaetz.

Abstract:

Determining how soft-tissues are preserved and persist through geologic time are continuing challenges because decay begins immediately after senescence while diagenetic transformations generally progress over days to millions of years. However, in recent years, carbonate concretions containing partially-to-fully decayed macroorganisms have proven to be remarkable windows into the diagenetic continuum revealing insights into the fossilization process. This is because most concretions are the result of biologically-induced mineral precipitation caused by

This article is protected by copyright. All rights reserved

the localized decay of organic matter which oftentimes preserve a greater biological signal relative to their host sediment. Here we present a comparative lipid biomarker study investigating processes associated with soft-tissue preservation within Holocene-age carbonate concretions that have encapsulated modern capelin (Mallotus villosus). We focus on samples collected from two depositional settings that have produced highly contrasting preservation end-members: 1) Kangerlussuaq, Greenland: a marine environment which, due to isostatic rebound, has exposed strata containing concretions exhibiting exceptional soft-tissue preservation (6 – 7 Kya), and 2) Greens Creek, Ottawa, Canada: a paleo brackish-to-freshwater marine excursion containing concretions exhibiting skeletal remains (~11 Kya). Lipid biomarker analysis reveal endogenous capelin tissues and productive waters at Kangerlussuaq that are in sharp contrast to Greens Creek concretions which lack appreciable capelin and environmental signals. Comparable distributions of bacterial fatty acids and statistical analyses suggest soft-tissue preservation within concretions is agnostic to specific heterotrophic decay communities. We therefore interpret preservation within carbonate concretions may represent a race between microbially-induced authigenic precipitation and decay. Namely, factors resulting in exceptional preservation within concretions likely include: 1) organic matter input, 2) rate of decay, 3) carbonate saturation, 4) porewater velocity, and 5) rate of authigenic (carbonate) precipitation resulting in arrested decay/bacterial respiration due to cementing pore-spaces limiting the diffusion of electron acceptors into the decay foci.

Key words: carbonate concretions, soft-tissue preservation, biomarkers, fossilization

1. Introduction

Determining how animal fossils form and the ways in which their soft-tissues are preserved in the geologic record has been a challenge to unravel because decay begins immediately after senescence while diagenetic alteration of organic matter continues over millions of years. Laboratory experiments running days to years provide important insights to some of the processes taking place (e.g., Allison, 1986; Briggs and Kear, 1993; Butler et al., 2015; Darroch et al., 2012; Gäb et al., 2020; Gupta et al., 2009; Iniesto et al., 2013; McCoy et al., 2015b; Naimark et al., 2016; Sansom et al., 2011). However, fossilization is ultimately the consequence of compounding factors, and this complexity poses various challenges for

This article is protected by copyright. All rights reserved

laboratory and modelling studies (Briggs, 1995; Briggs and McMahon, 2016; Parry et al., 2018; Purnell et al., 2018; Sansom, 2014). Pathways of organic matter preservation are thought to not only depend on its original composition (e.g., Sansom et al., 2011), but also contingent on the depositional setting (e.g., sedimentation rates, sedimentary composition, water chemistry, etc.) (Allison, 1988a; Elder and Smith, 1988), and the nature of microorganisms involved in decay (Allison, 1988b; Briggs, 2003; Gäb et al., 2020; Iniesto et al., 2017, 2015). Therefore, while taphonomic experiments have significantly advanced our understanding of soft-tissue preservation, it would be ideal if fossilization could be caught in the act under natural conditions.

In recent years, with the application of contemporary organic geochemistry techniques (e.g., gas chromatography-mass spectrometry), interest surrounding carbonate concretions has seen a resurgence as potential windows into the fossilization process or the 'diagenetic continuum' (Melendez et al., 2013a). Ubiquitous throughout the geological record, carbonate concretions are thought to be the result of biologically-induced (i.e., Dupraz et al., 2009) authigenic precipitation containing a range of partially-to-fully decayed macroorganisms as their nucleus (Clements et al., 2019; Coleman, 1993; Duan et al., 1996; Raiswell, 1976; Zatoń and Marynowski, 2004). Although concretions without obvious organic foci have also been described (e.g., McBride and Milliken, 2006). Specifically, their formation has been proposed to be the result of: 1) anaerobic microbial decay of an organic carbon source (e.g, a dead fish) resulting in 2) localized supersaturation of HCO_3^- ions which generate a pH and alkalinity gradient (i.e., microenvironment) that is 3) proportional to the rate of decay and diffusion resulting in 4) the decreased solubility (i.e., increased saturation index) and consequent microbially-induced carbonate precipitation (Berner, 1969; Berner, 1968; Coleman, 1993; Coleman and Raiswell, 1995, 1981; Mozley, 1996; Pye et al., 1990; Raiswell, 1976; Raiswell and Fisher, 2000).

Due to their frequent association with encapsulated organisms, concretions are particularly interesting for studying the fossilization of animal soft tissues (Thiel and Hoppert, 2018; Wilson and Brett, 2013). This is because authigenic mineral precipitation has been observed to entomb organic carbon sources within carbonate matrices ensuring its survival through diagenesis (Blumenberg et al., 2015; Brown et al., 2017; Grice et al., 2019; Mcnamara et al., 2009; Melendez et al., 2013a; Plet et al., 2017). Moreover, organomineralized and biomineralized carbonates (e.g., stromatolites, egg shells, seashells, coccoliths) have been shown

This article is protected by copyright. All rights reserved

to adsorb and encapsulate peptide sequences, polysaccharides, DNA, and lipids for timescales beyond their normal stability range (Crisp et al., 2013; Demarchi et al., 2016; Oskam et al., 2010; Sand et al., 2014). Mineral precipitation may also fractionate biomarkers into inter- and intra-crystalline species with varied degrees of diagenetic alteration (Ingalls et al., 2004). Therefore, carbonate concretions containing a discernable organic carbon source and low thermal maturity may be viewed as instances where the fossilization process has effectively been 'caught in the act' in its natural state (Thiel and Hoppert, 2018; Wilson and Brett, 2013). This notion is supported by work demonstrating concretions can preserve signals for the nucleating organism (Melendez et al., 2013b), diagenesis (Melendez et al., 2013a), and the sedimentary environment (Lengger et al., 2017; Thiel and Hoppert, 2018).

During the earliest steps of animal decay, autolysis by hydrolytic enzymes digest carbohydrates and proteins while labile organic compounds are quickly remineralized by heterotrophs (Butler et al., 2015; Gäb et al., 2020; Iniesto et al., 2017). Under aerobic conditions, these processes, along with bioturbation and scavenging, can result in the complete destruction of organic matter in sediments (Hedges and Keil, 1995, Sun et al., 1997; Lehmann et al., 2002). As the supply of oxygen is consumed by respiration, microorganisms then transition toward less-optimal terminal electron acceptors (e.g., SO_4^{2-}, Fe^{3+}) which effectively decrease rates of decay (Muscente et al., 2017, Andersen, 1996). However, this shift does not necessarily result in an increased preservation potential although anoxic conditions may restrict scavenging and permit the preservation of articulated body fossils under some settings (Allison, 1988a). Thereafter, recalcitrant materials (e.g., biomineralized tissue, lipids, and some polymers such as melanin) may survive due to selective preservation and/or diagenetic transformation into their stable counterparts and incorporations into macropolymers (Alleon et al., 2017; Briggs and Summons, 2014; Gupta et al., 2009; Larter and Douglas, 1980; Lindgren et al., 2012; Wiemann et al., 2018). Interestingly, taphonomic studies have suggested that communities responsible for decay may paradoxically be responsible for enhanced preservation (Allison, 1988b; Briggs, 2003; Darroch et al., 2012; Iniesto et al., 2013; Sagemann et al., 1999). For instance, sulfate-reducing bacteria (SRB) sustaining H_2S-rich conditions (i.e. euxinia) appear to have mediated the preservation of cholesterol and diagenetically modified derivatives for approximately 380 million years within a carbonate concretion (Melendez et al., 2013b). This has been inferred to be via 1) authigenic carbonate precipitation and subsequent encapsulation (Raiswell and Fisher, 2000), 2)

This article is protected by copyright. All rights reserved

sulfurization of lipids (Adam et al., 2000), and 3) abiotic H_2S-mediated hydrogenation (Hebting, 2006).

Despite advances understanding preservation mechanisms within concretions, the nature of biological activity in more recent settings affords an opportunity to identify biases relevant to the wider topic of animal soft-tissue and lipid biomarker preservation in the geological record. In this study, we investigate the role of biotic and abiotic mechanisms (e.g., decay, authigenic precipitation, water chemistry, sulfurization, etc.) on soft-tissue preservation within Holocene-age concretions which have encapsulated capelin (Mallotus villosus). Capelin are small forage fish which spend most of their life offshore and only enter coastal waters to spawn demersally or on gravely beaches, usually resulting is mass deaths (Nakashima, 2002). We compare and discuss biomarker results from two depositional settings that have produced fossils with contrasting degrees of soft-tissue preservation. The sites are:

Kangerlussuaq, Greenland: A marine environment where glacial sediments, recently exposed due to isostatic rebound (Dietrich et al., 2005; Storms et al., 2012), host concretions containing exceptional soft-tissue preservation (Bennike, 1997) (Figure 1a).

Greens Creek, Ottawa, Canada: Represents the sedimentary remains from the ephemeral brackish-to-freshwater Champlain Sea (Parent and Occhietti, 1988), a marine incursion episode which harbors concretions mostly containing articulated skeletal remains (Gadd, 1980) (Figure 1b).

The samples from these sites are thermally unaltered carbonate concretions found shallowly buried in sediments which are similar with respect to the nucleating organic carbon source (i.e., capelin) and relative age (Bennike, 1997; Gadd, 1980). Differences in preservation states may therefore be attributable to their contrasting depositional settings which potentially host varying heterotrophic microbial communities. These fossils thus serve as approximate fossilization experiments under natural conditions to investigate the result of contrasting conditions and underlying soft-tissue preservation mechanisms.

2. Materials and Methods

2.1. Site description and sample collection

Kangerlussuaq, Greenland: The Kangerlussuaq fjord (Danish: Søndre Strømfjord) is a marine environment flanked by highly reworked Archean gneisses inhabited by various species of

This article is protected by copyright. All rights reserved

vascular plants and lichens encompassing its modern catchment (Henkemans et al., 2018). The present-day depth varies between a few meters by the Kangerlussuaq airport (SFJ) near uplifted sediments where concretions have been collected to over 300 meters where the mouth of the fjord meets the Davis Strait. During the early Holocene, sea level was approximately 40 meters above the present-day land surface at the head of fjord in this paleo tidewater glacier environment. Eventually, it experienced relative sea level decline due to isostatic rebound as the Greenland Ice Sheet (GIS) retreated at the end of the Last Glacial Maximum (LGM) (Dietrich et al., 2005; Storms et al., 2012). This is important because, during deglaciation periods, fjords (and glacial valleys) usually become major sediment sinks due to glacier-induced mass wasting. This results in significant influxes of terrigenous organic matter and nutrients into the water column often inducing eutrophic conditions and bottom water anoxia (Smittenberg et al., 2004). The concretion studied here was collected southwest of the Kangerlussuaq airport at the head of the fjord (c.1960 by Lise Lawaetz) from uplifted sandy glacial sediments where a suite of marine and land vertebrate fossils have been reported by Bennike, 1997 (67°00'06.8"N 50°46'19.8"W) (Supplementary Figure 1).

Greens Creek, Ottawa, Canada: As the Laurentide ice sheet continued its retreat beyond the Canadian shield from its furthest extent during the LGM, freshwater proglacial Lake Candona was breached by intruding marine waters from the Goldthwait Sea in the isostatically depressed St. Lawrence Valley ~12,400 years ago (Parent and Occhietti, 1988). This event resulted in the ephemeral marine phase recognized as the Champlain Sea which stood up to 230 meters above the present-day Ottawa/Montreal/Burlington region. However, isostatic rebound resulted in the retreat of marine waters ~10,000 years ago followed by the emplacement of modern Lake Champlain (Parent and Occhietti, 1988). Work on depositional facies near Montreal indicate that waters were approximately a mixture of 33% marine and 67% glacial meltwater (Desaulniers and Cherry, 1989) resulting in brackish-to-freshwater (and possibly estuarine) conditions as previously suggested by the presence of freshwater-tolerant fish fossils at Greens Creek (e.g., capelin, stickleback, sculpin) (McAllister et al., 1981). Palynological analysis of concretion matrices and the discovery of a rare, leopard frog concretion (Rana pipiens), indicate the paleo catchment supported shrub tundra communities (Holman et al., 1997). Canadian capelin concretions were generously provided by the Geological Survey of

This article is protected by copyright. All rights reserved

186 Canada collected from Greens Creek clays derived from the ephemeral Champlain Sea
187 (45°27'56.6"N 75°34'34.7"W) (GSC loc. 60327) (Supplementary Figure 1).
188 Samples from both locations have been determined to be Holocene-age through ^{14}C
189 radiocarbon dating techniques (Table 1). Capelin concretions from Kangerlussuaq are about
190 6000 - 7000 years old (Brink, 1975) while concretions from Greens Creek have been dated at
191 10,780 ± 80 years old (Gadd, 1980). Modern capelin, our analytical reference control, were
192 acquired from the Denmark Strait (Icelandic^{+} Capelin Whole Fish).
193
194 2.2. Sample preparation
195 Concretions were prepared in accordance to similar methods implemented by Melendez et al.,
196 (2013a). Approximately 10 mm of each concretion's exposed outer surface was removed by
197 abrading with a Dremel rotary (model 8220-1/28) and diamond cut-off wheel (McMaster-Carr,
198 1257A33). Approximately ~2 mm thick slices oriented parallel to the fossil nucleus were then
199 taken yielding 4 layers for each specimen (Figure 2). The slices are the fossil layer, matrix 1,
200 matrix 2, and the concretion rim (Figure 2). Biomarker discussions from Greenland and Canada
201 shown here represent analysis from the fossil layer and matrix 1, respectively. These selections
202 were made because of the presence of a carbonaceous film in the Greenland fossil layer while
203 only trace lipids were detected in the Canada fossil layer. Matrix 1 was selected due to its
204 proximity to the nucleus and abundance of detectable compounds. Slices were crushed in a Spex
205 8510 Shatterbox with a mill and puck cleaned with solvents (i.e., methanol, dichloromethane -
206 DCM, n-hexane) and combusted sand (12 hours at 850 °C) between samples. Recently dead
207 capelin were segmented into different components including the head, tail, internal organs
208 (including heart, stomach, etc.), stomach only, whole fish with internal organs, and whole fish
209 without organs. These were then ground with a tissue homogenizer. All tools (except the Dremel
210 rotary) were solvent cleaned five-times with methanol and DCM and combusted at 550 °C for 12
211 hours while glassware underwent two dishwasher cycles prior to being combusted at 550 °C for
212 12 hours prior to usage. Lipid extractions described below were accompanied by solvent and
213 extraction blanks to determine potential sources of contaminants (if any).
214
215 2.3. Extraction of free lipids (inter-crystalline)

This article is protected by copyright. All rights reserved

An internal standard (2 µg of 3-methyltricosane) was added to all samples prior to extraction for calculating extraction efficiency. Up to 5 grams of the crushed concretion samples were solvent-extracted using a Dionex Accelerated Solvent Extraction (ASE) 350 with DCM-methanol (9:1, v/v) programmed with the following method: cell volume - 34 mL, oven temperature – 100 ºC, oven heat – 5 minutes, static time – 15 min, static cycles – 3, flush volume – 130 %, purge time – 100 seconds. Homogenized modern tissue samples (~1 mg each) were solvent-extracted with 25 mL DCM-methanol (9:1, v/v) via sonication in 50 mL glass vials in order to prevent probable cross-contamination from organic-rich samples in the ASE. All extracted samples were concentrated to ~ 1mL under a steady nitrogen stream on a Zymark Turbovap LV evaporator then transferred into 2 mL vials to evaporate overnight inside an empty fume hood. Dry total lipid extracts (TLEs) were methylated by adding 100 µL of 0.5 N methanolic-HCl (Sigma Aldrich, 07607) to 2 mL vials which were then tightly capped and heated for 16 hours at 60 ºC in order to convert glycerides and free fatty acids (not to be confused with inter-crystalline free lipids) into fatty acid methyl esters (FAMEs). Derivatized samples were cooled, 100 µL of five-times DCM-cleaned Milli-Q water was then added to quench the reaction and permit extraction from the aqueous phase with 4:1 (v/v) n-hexane-DCM. The (top) organic phase was transferred into 2 mL GC vials with inserts for GC-MS. Samples were concentrated under a gentle nitrogen stream and resuspended in 100 µL n-hexane to be analyzed, 50% (50 µL) was taken to be fractionated by column chromatography.

2.4. Extraction of carbonate-bound lipids (intra-crystalline)

ASE extraction residues from the concretion samples were placed in 500 mL beakers and dissolved by the gradual addition of DCM-washed 2N hydrochloric acid to release intra-crystalline lipids (O'Reilly et al., 2017). Once dissolution was complete, solutions were diluted with DCM-cleaned water and extracted five times with DCM in a 500 mL separatory funnel by liquid-liquid extraction. As above, the carbonate TLEs were methylated (16 hours at 60 ºC) and split for column chromatography.

2.5. Copper desulfurization (elemental sulfur removal)

Elemental sulfur (only detected in Greenland TLE chromatograms as a broad hump dominated by m/z 64) was removed by incubating the TLEs with 1 g of activated-copper shavings in 4 mL

This article is protected by copyright. All rights reserved

glass vials for 2 hours at room temperature. Additional shavings were added if most of the copper darkened due to reacting with sulfur. TLEs were then recovered by rinsing the glass vial five times with DCM.

2.6. Raney nickel desulfurization (sulfur-bound lipid extraction)

Freshly extracted (i.e., additional subsamples from concretion slices) Greenland TLEs (not Cu-treated as above) underwent Raney nickel (RN) desulfurization in order to liberate (potentially) sulfur-bound lipids (Sinninghe Damsté et al., 1988). TLEs, initially ASE extracted in 9:1 DCM:MeOH, were gently dried and resuspended in 100 µL distilled absolute ethanol (EtOH >99.5%) to be transferred into 500 mL conical flasks, each coupled to an Allihn condenser. Five 9-inch glass Pasteur pipette volumes (~10 mL) of RN were added to each conical flask and the reaction was heated to 80 ºC for 2 hours and continuously mixed via a magnetic stir bar. The system was kept anaerobic with a constant nitrogen stream in order to prevent the RN reacting with atmospheric O_2. Desulfurized TLEs were then extracted five times with DCM (liquid-liquid) being careful to avoid the RN becoming dry before deactivation. Subsequently, the non-polar fractions of the desulfurized TLEs were fractionated according to the method below.

2.7. Column chromatography

TLE splits (free, carbonate-bound, and RN-desulfurized) were fractionated using column chromatography on ~5 g of deactivated silica gel (2% wt H_2O). Three fractions were collected: F1 (saturated hydrocarbons) eluted with 2 dead volumes (DV) of n-hexane; F2 (FAMEs and aromatics) eluted with 3 DV of 1:1 (v/v) n-hexane:DCM; F3 (polar lipids) eluted with 2 DV 4:1 (v/v) DCM:MeOH and 1 DV MeOH. F3 samples were concentrated under a gentle nitrogen stream to be derivatized in 25 µL pyridine and 25 µL N,O-Bis(trimethylsilyl)trifluoro-acetamide with trimethylchlorosilane (i.e., BSTFA+TMCS; Sigma Aldrich, 15238) for 1 hour at 70 ºC immediately prior to GC-MS analysis. Raney nickel desulfurized TLEs were separated into two fractions: F1 RN (non-polar lipids) with 4 DV 9:1 n-hexane:DCM; F2 RN (polar lipids) with 4 DV 4:1 DCM:MeOH. All fractions, excluding F3 (to be derivatized by BSTFA/pyridine), were concentrated and resuspended in 50 µL n-hexane to be analyzed by GC-MS.

2.8. Gas chromatography-mass spectrometry

This article is protected by copyright. All rights reserved

Aliquots of the methylated TLEs and subsequent fractions from column separations (F1 – F3, F1 RN) were analyzed on an Agilent 6890A gas chromatograph (GC) interfaced with an Agilent 5975C (MS). The GC was equipped with a programable temperature vaporizer (PTV) inlet (Gerstel) held at 300 ºC and a J&W DB-5MS fused silica capillary column (60 m x 0.25 mm x 0.25 µm) programmed with the following parameters: 60 °C injection and hold for 2 min, ramp at 10 °C min^{-1} to 140 °C, followed directly by a ramp at 3.5 °C min^{-1} to 320 °C, and a final isothermal hold at 320 °C for 33.6 min.

The MS source was set to 230 °C, the quadrupole was set to 150 °C, and the MS was operated in electron impact (EI) mode at 70 eV with a scan range between m/z 50 to 580. Results were analyzed using Agilent MassHunter Qualitative B.08.00. All reported compounds were identified using a combination of C_8 – C_{40} n-alkane standards (Sigma Aldrich, 40147-U), $C_{4:0}$ – $C_{24:0}$ FAME standards (Sigma Aldrich, 18919-1AMP), steroid standards (e.g., sterol, stanols), mass spectral libraries (NIST17), interpretation of fragmentation patterns, retention times, and comparison to reference literature. Fatty acid identifications were supplemented using a modern capelin tissue reference (Supplementary Figure 2) and work on fish lipids (Sigurgisladóttir and Pálmadóttir, 1993). Branched-chain fatty acids (BCFA) were identified using fragment ions formed by cleavages adjacent to branch-points as determined by Ran-Ressler et al., 2012. Sterol/stanol identifications were supplemented using fragmentation patterns compiled by Prost et al., 2017.

2.9. Gas chromatography isotope-ratio mass spectrometry

Compound specific carbon isotope ratios of n-alkanes (F1) and major fatty acids (F2) were measured on a Trace 1310 gas chromatograph coupled to a MAT253 isotope ratio mass spectrometer (GC-IRMS) (Thermo Fisher) via a combustion furnace containing copper, nickel, and platinum wires operated at 850 °C. The GC was equipped with a PTV injector and a J&W DB-1MS column (60 m x 0.24 mm x 0.25 µm). Measurements were performed in triplicate and are reported in delta notation ($\delta^{13}C$ in per mil, ‰) against Vienna Pee Dee Belemnite. Carbon isotope ratios were corrected for changes in linearity and reproducibility with an n-alkane mixture standard (A5, Arndt Schimmelmann, Indiana University) injected after every sample replicate group. The standard deviation for the instrument, based on replicate standard injections,

This article is protected by copyright. All rights reserved

was below 0.4‰. We report data from all concretion slices, albeit, for well-resolved analytes only.

2.10. Multivariate analysis

Principal component analysis (PCA) is a multivariate statistical method for identifying patterns within large data sets of correlated variables (Hotelling, 1933). PCA has been previously used to identity classes of fossilized tissue (Fabbri et al., 2020; McCoy et al., 2020; Wiemann et al., 2020, 2018) and factors affecting soft-tissue preservation within concretions (McCoy et al., 2015b). We accordingly implement PCA to identify potential relationships between lipid source and preserved soft-tissues. Fatty acids detected in modern capelin along with free and carbonate-bound lipids across all slices (i.e., fossil layer, matrix 1, matrix 2, rim) were defined as variables. Only methylated and diagenetically unaltered fatty acids identified in F2 fractions from column separations were selected for consistency. Therefore, α,ω-dicarboxylic fatty acids and hydroxy fatty acids (which have also been silylated in F3) were not included. The area under each compound (peak) in the total ion chromatogram (TIC), normalized to total organic carbon (g) (see below), was determined using an automated integration script curated with retention times on the Agilent Quantitative Analysis (for GC-MS) B.08.00 software. PCA was executed on GraphPad Prism 9.1.1 software.

2.11. Bulk composition by loss on ignition

Bulk weight percent total organic carbon and carbonate contents of all concretion slices (fossil, matrix layers, and rim) were estimated by loss on ignition (LOI). 500 mg of each (crushed) concretion slice was weighed on a small ceramic crucible and combusted inside a Barnstead/Thermolyne 30 400 furnace at 550 ºC for 4 hours. Once the samples cooled, the crucibles were re-weighed, and the mass loss was inferred to be the TOC. Samples were re-combusted at 950 ºC for 2 hours, and the subsequent mass loss was inferred to be predominantly from calcium carbonate converted to CaO.

2.12. Thin sections and targeted electron microprobe analysis

Concretion thin sections, perpendicular to the fossil nucleus (as defined in section 2.2.), were prepared on a Struers Accutom-100 for imaging and elemental analysis at the MIT Electron

This article is protected by copyright. All rights reserved

Microprobe Facility. Thin sections were first photographed on a Zeiss AX10 followed by targeted mineral identification on a JEOL-JXA-8200 Superprobe at a 2-micron aperture.

3. Results

3.1. Bulk composition

The total organic carbon of the Greenland and Canada fossil layers were indistinguishable at 5.5%. The carbonate contents were also similar, 57% Greenland and 55% Canada (Table 1). Results for all concretion slices (Greenland & Canada) are found in Table 1.

3.2. Thin sections and mineral identifications

Both Greenland and Canada thin sections reveal micritic concretion matrices containing sparse detrital inclusions (Supplementary Figure 3). The Greenland concretion displays irregular radial laminations which alternate between light and dark bands whereas no laminations were observed in the Canada concretion (Supplementary Figure 3). The Canada concretion contains detrital quartz, dolomite, and epigenetic manganese dendrites (Seilacher, 2001) while the Greenland concretion contains quartz, apatite, and sulfur-rich amorphous organics (Supplementary Figure 3, 4).

3.3. Saturated hydrocarbons

n-Alkanes (C_{17} – C_{40}) were the predominant saturated hydrocarbons detected from Greenland free lipids (GFL) and carbonate-bound (GCB) fractions along with Canada free lipids (CFL) and carbonate-bound (CCB) fractions (Figure 3). GFL displayed an odd-carbon number preference for long-chain (C_{20} – C_{37}) n-alkanes with a maximum (C_{max}) at C_{27} (Figure 3a), GCB did not display a carbon preference and had a C_{max} at C_{29} for long-chain n-alkanes (Figure 3a). CFL displayed a C_{max} at C_{18} for short-chain n-alkanes (C_{17} – C_{20}), odd-carbon preference and C_{max} at C_{27} for long-chain n-alkanes, and CCB did not display a carbon preference while having a C_{max} at C_{29} (Figure 3b). Calculated pristane/phytane (Pr/Ph) ratios spanning all slices from the fossil layer towards the outer rim were between 0.3 – 0.4 in GFL and 0.6 – 1 in CFL samples (Figure 4a). Pristane and phytane could not be detected in the carbonate-bound fractions. Carbon preference index (CPI) (Bray and Evans, 1961) values ranged between 1.94 – 3.6 for GFL, 1 – 1.1 for GCB, 2.3 – 3.5 for CFL, and 1.4 – 1.5 for CCB (Figure 4b). Terrestrial-aquatic ratios for

This article is protected by copyright. All rights reserved

hydrocarbons (TAR_{HC}) (Meyers, 1997) ranged between 7.8 – 50 for GFL, 100 for GCB, 0.1 – 0.2 for CFL, and 9.3 – 18 for CCB (Figure 4c). Total ion chromatograms are available in Supplementary Figure 5.

3.4. Fatty acids

Lipid extracts from modern capelin tissues (e.g., tail, with internal organs, stomach only, etc.) yielded the same major fatty acids as those present in muscle (Supplementary Figure 2), albeit, at varying relative abundances. Fatty acids from Greenland were abundant and diverse in structure. Straight-chain ($C_{14:0}$ – $C_{30:0}$), branched-chain (BCFA) ($C_{14:0}$ – $C_{17:0}$), monounsaturated (MUFA), and polyunsaturated (PUFA) fatty acids were all detected in GFL (Figure 5a, Table 2) while similar compounds, except for unsaturated fatty acids, were also detected in GCB (Figure 5a, Table 2). GFL long-chain ($C_{20:0}$ – $C_{30:0}$) fatty acids displayed an even-carbon preference with a C_{max} at $C_{24:0}$ (Figure 5a), GCB displayed a similar carbon-preference with a C_{max} at $C_{20:0}$ (Figure 5a). Fatty acids from CFL exhibited a comparable diversity to GFL. $C_{14:0}$ – $C_{30:0}$ straight chain fatty acids, long-chain fatty acids ($C_{20:0}$ – $C_{30:0}$) with a C_{max} at C_{24}, BCFAs ($C_{15:0}$ – $C_{17:0}$), and MUFAs were all detected (Figure 5b, Table 2). Straight-chain saturated $C_{14:0}$ - $C_{18:0}$ and $C_{15:0}$ BCFA were the only fatty acids detected in CCB (Figure 5b, Table 2). Both GFL and CFL contained compounds found in modern capelin soft-tissue ($C_{14:0}$, $C_{16:0}$, $C_{18:1\omega9}$, $C_{18:0}$) whereas $C_{18:2\omega6}$, $C_{18:1\omega7}$, $C_{20:1\omega9}$, and $C_{22:1\omega9/11}$ were only detected in GFL (Table 2). $C_{16:1\omega7}$ was the single major monoenoic fatty acid from modern capelin not detected in any concretion sample (Table 2). Terrestrial-aquatic ratios for fatty acids (TAR_{FA}) (Meyers, 1997) were between 0.1 – 0.3 for GFL, 0 – 0.4 for CFL, and were 0 for both GCB and CCB (Figure 4d). Notable similarities between Greenland and Canada include: 1) homologous long-chain fatty acid distribution with C_{max} at C_{24}, and 2) detection of 3-Me$C_{16:0}$, 8-Me$C_{16:0}$, 10-Me$C_{16:0}$, 2-Me$C_{16:0}$, 15-Me$C_{16:0}$, and 14-Me$C_{16:0}$ (i.e., branched $C_{17:0}$) BCFAs in GFL, GCB, and CFL. In addition, an abundance of hydroxy fatty acids (OHFA) were detected in Greenland polar fractions, GFL and GCB, including β-OHFA, α-OHFA, and ω-OHFA. β-OHFA dominated between $C_{14:0}$ and $C_{18:0}$ in GFL, while α-OHFA were more prominent between $C_{22:0}$ and $C_{30:0}$ (Supplementary Figure 7). ω-OHFA were only detected in $C_{16:0}$ and $C_{22:0}$ carbon lengths in GFL (Supplementary Figure 7). Lastly, α,ω-dicarboxylic fatty acids (DCFA) were detected in both GCB and CCB (Table 2). Total ion chromatograms are available in Supplementary Figure 6.

This article is protected by copyright. All rights reserved

401

402 3.5. Multivariate analysis of fatty acids

403 Principal component analysis (PCA) performed using fatty acids as variables (excluding hydroxy
404 and dicarboxylic acids) detected 17 PC axes, with the first three explaining more than 15% of
405 variation and 98% of the total variability (Figure 6, Supplementary Figure 7). PCA biplots for
406 the first three axes simultaneously represent samples and how strongly each variable influences
407 the principal component (Figure 6). Samples are designated as above (i.e., GFL, GCB, CFL,
408 CCB), however, all concretion slices have been included for analysis. The nomenclature used is
409 the following: M1 – modern capelin tissue (female), M2 – modern capelin tissue (male), 0 –
410 fossil layer, 1 – matrix 1, 2 – matrix 2, 3 – rim. For example, GFL0 – Greenland fossil layer free
411 lipids and CCB2 – Canada matrix 2 carbonate-bound lipids. Variance in PC1 is explained by
412 branched $C_{15:0}$ (13Me$C_{14:0}$, 12Me$C_{14:0}$), branched $C_{17:0}$ (3-Me$C_{16:0}$, 8-Me$C_{16:0}$, 10-Me$C_{16:0}$, 2-
413 Me$C_{16:0}$, 15-Me$C_{16:0}$, and 14-Me$C_{16:0}$), and $C_{19:0}$ – $C_{30:0}$ straight chain fatty acids (Figure 6a,
414 Supplementary Figure 7). Variance in PC2 is explained by unsaturated fatty acids found in
415 modern capelin tissue ($C_{14:0}$, $C_{16:0}$, $C_{16:1\omega9}$, $C_{18:1\omega9}$, $C_{18:1\omega7}$, $C_{20:1\omega9}$, $C_{20:1\omega7}$, $C_{22:1\omega7}$) (Figure 6a,
416 Supplementary Figure 7). Variance in PC3 is explained by branched $C_{15:0}$ (2Me$C_{14:0}$), branched
417 $C_{16:0}$ (14Me$C_{15:0}$), and unsaturated fatty acids ($C_{14:1\omega5}$, $C_{15:1\omega9}$, $C_{16:1\omega5}$) (Figure 6b, Supplementary
418 Figure 7).

419

420 3.6. Polar lipids

421 Following hydrolysis, the lipid extracts from modern capelin tissue samples yielded identical
422 profiles, in this case, cholesterol was the only compound detected (Supplementary Figure 8).
423 GFL was primarily composed of C_{12} – C_{32} fatty alcohols (n-alkanols) with a C_{max} at $C_{22,}$ C_{21} –
424 C_{25} alkan-2-ols, and phytol (Table 2, Supplementary Figure 7). Major sterols detected in GFL
425 were cholesterol and β-sitosterol along with minor stigmasterol and campesterol. Stanols
426 detected in GFL were coprostanol, epicoprostanol, cholestanol, 5β-stigmastanol, epi-5β-
427 stigmastanol, and 5α-stigmastanol (Table 2, Supplementary Figure 7). Moreover, C_{30} – C_{32}
428 hopanoids and triterpenoids (i.e., β-amyrin and α-amyrin) were also detected (Table 2,
429 Supplementary Figure 9). In general, compounds in GCB mirrored GFL except for
430 epicoprostanol, campesterol, and C_{30} – C_{31} hopanoids (Table 2). C_{24}, C_{26}, and C_{28} n-alkanols and

This article is protected by copyright. All rights reserved

cholesterol were identified in trace amounts in CFL, no polar lipids were identified in CCB (Table 2).

3.7. Raney nickel

RN desulfurized non-polar lipids are dominated by long-chain (C_{21} – C_{40}) n-alkanes with a C_{max} at C_{26} and a series of methyl-branched alkanes (Supplementary Figure 10). Aryl isoprenoids and carotenoids diagnostic of sulfur-oxidizing bacteria were not detected (Supplementary Figure 10).

3.8. $\delta^{13}C$ measurements

No corrections were made for the single carbon added by methylation of the fatty acids as experiments with internal standards did not reveal a measurable impact. Saturated hydrocarbon isotope values from GFL, GCB, and CFL varied from -29 to -32‰ without defined structure (Figure 7). Measurements from all samples appear to resemble each other across carbon length, site (Greenland vs. Canada), and source (free vs. carbonate-bound) (Figure 7). Short-chain ($C_{14:0}$ – $C_{18:0}$) and monoenoic fatty acid carbon isotope values from GFL, GCB, and CFL varied between -24 to -30‰, in contrast, long-chain ($C_{19:0}$ – $C_{30:0}$) fatty acid measurements for GFL and GCB varied between -28 to -32‰ (Figure 8).

4. Discussion

4.1. Results overview

Two concretions from glacial environments (marine vs. brackish-to-freshwater), comparable age, and similar organic carbon sources (capelin) have produced highly contrasting fossil end-members (soft-tissue present vs. no soft-tissue) (Figure 1). Due to their relatively young age and shallow burial depths, thermal diagenesis is inferred to have been negligible. Thus, these concretions serve as approximate fossilization experiments found under natural conditions. Lipids extracted from the concretion free fraction (inter-crystalline) appear to be derived from more diverse (and possibly geologically recent) organic sources (e.g., vascular plants, algae, sulfate-reducing bacteria) (Table 2) (Ackman et al., 1968; Bianchi and Canuel, 2011; Drenzek et al., 2007; O'Reilly et al., 2017; Rielley et al., 1991; Volkman et al., 1980). In contrast, carbonate-bound lipids (intra-crystalline) have a relatively lower diversity and exhibit more

This article is protected by copyright. All rights reserved

462 diagenetically altered byproducts (e.g., dicarboxylic acids, stanols, loss of carbon preference)
463 which may coincide with carbonate precipitation/concretion growth (Table 2) (Bray and Evans,
464 1961; Volkman, 2016). Results from all concretion slices are reported in Supplementary Figures
465 11 – 15.
466
467 4.2. Greenland lipid sources & paleoenvironmental conditions
468 Vascular plant lipids: GFL long-chain (C_{20} – C_{37}) n-alkanes containing an odd-carbon preference
469 and C_{max} at C_{27} represent a predominant input from land plant leaf waxes (Figure 3a) (Eglinton
470 and Hamilton, 1967). Long-chain ($C_{20:0}$ – $C_{30:0}$) even-carbon preference fatty acids (Figure 5a)
471 and triterpenoid alcohols (i.e., amyrin) in both GFL and GCB (Table 2) further suggest input
472 from vascular plants (Bianchi and Canuel, 2011; Řezanka, 1989; Rielley et al., 1991).
473 Accordingly, $\delta^{13}C$ values between -29 to -32‰ for n-alkanes (C_{20} – C_{37}) (Figure 7) and -28 to -
474 32‰ for fatty acids ($C_{19:0}$ – $C_{30:0}$) (Figure 8) typical for C3 plants appear to confirm this
475 interpretation (Drenzek et al., 2007; Volkman, 2006). Interestingly, the lack of carbon preference
476 in GCB n-alkanes (Figure 3a) and C_{max} at C_{29} may indicate contribution from a catchment-
477 derived mature hydrocarbon (Bray and Evans, 1961). CPI values (Figure 4b) further demonstrate
478 contrasting terrestrial sources have been incorporated into the free lipid (GFL > 1) and carbonate
479 fractions (GCB = 1) (Bray and Evans, 1961). High TAR_{HC} ratios at Greenland indicate greater
480 terrestrial (i.e., vascular plants) hydrocarbon contribution versus aquatic (i.e., algal & bacterial)
481 (Figure 4c).
482 Algal lipids: C_{28} – C_{29} phytosterols (campesterol, stigmasterol, and sitosterol), branched
483 $C_{16:0}$ (14Me$C_{15:0}$), monounsaturated fatty acids ($C_{14:1\omega5}$, $C_{15:1\omega9}$, $C_{16:1\omega5}$, $C_{17:1\omega9}$), and fatty
484 alcohols (n-alkanols) suggest contribution and enhanced primary productivity by microalgae
485 (Ackman et al., 1968; Volkman, 2006; Volkman et al., 1998, 1980). TAR_{FA} ratios indicate
486 greater aquatic contributions of fatty acids (Figure 4d) (Meyers, 1997).
487 Bacterial lipids: Short-chain fatty acids ($C_{14:0}$ – $C_{19:0}$) detected in both GFL and GCB
488 (along with the presence of elemental sulfur in chromatograms m/z 64) suggest a close
489 association with sulfate-reducing bacteria (SRB). Branched $C_{17:0}$ fatty acids (Table 2), namely,
490 10-Me$C_{16:0,}$ are particularly diagnostic for Deltaproteobacteria (Dowling et al., 1986; Taylor and
491 Parkes, 1983) and have been identified in cultures of Desulfobacter and in areas harboring
492 persistent SRB communities (Elvert et al., 2003; Hinrichs et al., 2000).

This article is protected by copyright. All rights reserved

493 Paleoenvironment: Altogether, lipid biomarker results are comparable to contemporary
494 eutrophic fjords (e.g., Smittenberg et al., 2004). Bottom waters at Kangerlussaq were most likely
495 reducing (Figure 4a, Pr/Ph: 0.3 – 0.4) and sulfidic maintained by enhanced biological sulfate-
496 reduction in response to glacier-induced mass wasting (and organic matter input). The lack of
497 detectable aromatic carotenoids, however, does not indicate sulfidic conditions in the photic zone
498 (Supplementary Figure 10) (Melendez et al., 2013b). PCA results indicate variance in GFL
499 samples (e.g., fossil layer to rim) is best explained by a mixture of algal lipids and capelin soft-
500 tissue (Figure 6b).
501
502 4.3. Canada lipid sources & paleoenvironmental conditions
503 Vascular plant lipids: Like Greenland, CFL long-chain (C_{20} – C_{37}) n-alkanes containing an odd-
504 carbon preference and C_{max} at C_{27} likely represent input from land plants (Figure 3b) (Eglinton
505 and Hamilton, 1967). CCB trace hydrocarbons (like GCB) with an apparent lack of carbon
506 preference and C_{max} at C_{29} indicates a mature hydrocarbon input from the surrounding catchment
507 (Figure 3b) (Figure 3a) (Bray and Evans, 1961). CPI values for CFL and CCB mirror those of
508 GFL and GCB suggesting terrestrial sources with contrasting maturities have been incorporated
509 into free and carbonate-bound fractions. Homologous long-chain ($C_{20:0}$ - $C_{30:0}$) even-carbon-
510 number preference fatty acids with C_{max} at $C_{24:0}$ (Figure 5b) and $\delta^{13}C$ values consistent with C3
511 plants support input from terrestrial vascular plants (Figure 8) (Bianchi and Canuel, 2011;
512 Řezanka, 1989; Rielley et al., 1991). Still, we note that others have attributed this fatty acid
513 pattern to a microbial source (Řezanka 1990; Summons et al., 2013).
514 Algal lipids: TAR_{HC} and TAR_{FA} ratios (< 1) both indicate greater aquatic contributions
515 (algal & bacterial) over terrestrial (Meyers, 1997). However, CFL short-chain n-alkanes (C_{17} –
516 C_{20}) exhibit an unusual C_{max} at C_{18} possibly attributable to sulfate-reducing bacteria (discussed
517 below). C_{17} to C_{20} $\delta^{13}C$ values between -29 to -32‰ could represent a likely mixed bacterial-
518 algal source (McKirdy et al., 2010; Volkman, 2006). Phytosterols and unsaturated fatty acids
519 diagnostic of aquatic inputs are absent in both CFL and CCB (Table 2). Only C_{24}, C_{26}, and C_{28} n-
520 alkanols were identified in CFL (Table 2) (Volkman et al., 1998).
521 Bacterial lipids: CFL hydrocarbons display an unusual C_{max} at C_{18} which have previously
522 been attributed to bacterial origins in marine sediments (Aloulou et al., 2010; Grimalt and
523 Albaigés, 1987; Nishimura and Baker, 1986). Work by Davis, 1968 demonstrated that cultures of

This article is protected by copyright. All rights reserved

524 the sulfate-reducing bacterium Desulfivibrio desulfuricans produce comparable n-alkane profiles,
525 however, unusual n-alkane distributions have also been detected from other marine bacteria and
526 algae (Han and Calvin, 1969). In this instance, the cooccurrence of branched $C_{17:0}$ BCFA in CFL
527 and CCB suggest a likely association with sulfate-reducing bacteria like in Greenland (Figure 5,
528 Table 2) (e.g., Dowling et al., 1986; Taylor and Parkes, 1983).
529 Paleoenvironment: Given the dearth of lipid biomarker information, we are unable to
530 clearly establish environmental conditions at time of concretion formation. Pristane/phytane
531 values indicate possibly reducing bottom waters (anoxic) (Figure 4a) which are required to
532 prevent scavenging and permit the preservation of fully articulated fish remains (Allison, 1988a;
533 McAllister et al., 1981). Hydrogeological studies of clays, minerals, and porewaters emplaced
534 during the Champlain Sea suggest widespread occurrence of sulfate-reduction as pyrite and
535 HCO_3^- concentrations in saturation have been recorded (Desaulniers and Cherry, 1989b).
536 However, SRB activity would have most likely been attenuated by low SO_4^{2-} concentrations
537 which are predicted to have approached zero due to dilution from seasonal glacial discharge
538 (Cronin et al., 2008). Lipid biomarker results appear more consistent with low productivity
539 (pelagic) waters or perhaps generally reflect the decreased preservation potential at Greens
540 Creek. PCA results indicate variance in CFL samples is best explained by bacterial and
541 environmental lipids (Figure 6).
542
543 4.4. Hypotheses for mechanisms resulting in soft-tissue preservation
544 The diverse assemblage of lipids identified in this study, morphological features, and the
545 detection of nearly all lipids found in the reference capelin (except for $C_{16:1\omega7}$) demonstrate that
546 the Greenland concretion is an example of exceptional soft-tissue preservation (Figure 1, 5, 6).
547 This contrasts with the Canada concretion which is mostly devoid of soft tissue and is
548 overrepresented by environmental and bacterial signals (Figure 1, 5, 6). At Kangerlussuaq,
549 Greenland, sulfate-reducing bacteria (SRB) appear to be the principal mediators of concretion
550 formation under a eutrophic regime induced by glacial mass wasting. Aquatic and terrestrial
551 lipids are characterized by long-chain n-alkanes, monounsaturated fatty acids, polyunsaturated
552 fatty acids, long-chain fatty acids, hydroxy fatty acids, n-alkanols, phytosterols, and triterpenoids
553 (Table 2). At Greens Creek, although SRB lipids have been identified, it remains unclear
554 whether additional microbial communities were involved in concretion formation and how

This article is protected by copyright. All rights reserved

555 productive waters may have been. Using the presented data, we propose preservation biases
556 within concretions can be determined by evaluating two alternate hypotheses which weigh the
557 importance of specific bacterial communities (i.e., sulfate-reducing bacteria) versus depositional
558 parameters on exceptional preservation:
559 I: Enhanced preservation occurs due to SRB activity resulting in euxinic conditions
560 which result in H_2S-lipid interactions that impart labile compounds resistance to decay (Adam et
561 al., 2000; Hebting, 2006; Melendez et al., 2013b, 2013a).
562 II: Enhanced preservation occurs due to depositional parameters (e.g., primary
563 productivity, organic matter input, sediment porosity, diffusion, porewater velocity, and solute
564 concentrations) which determine favorable alkalinity gradients and mediate the rate of carbonate
565 precipitation (Berner et al., 1970; Berner, 1968a, 1968b). That is, exceptional soft-tissue
566 preservation within concretions may fundamentally represent a race between carbonate
567 precipitation and decay (Sagemann et al., 1999).
568
569 4.5. Controls on capelin soft-tissue preservation at Greenland and Canada
570 Taphonomic experiments have suggested that microbial communities involved in decay
571 may paradoxically be responsible for increased preservation (e.g., Allison, 1988b; Briggs, 2003;
572 Briggs and Kear, 1993; Briggs and McMahon, 2016; Butler et al., 2015; Gäb et al., 2020; Iniesto
573 et al., 2013; Sagemann et al., 1999). Early microbial colonization and production of biofilms
574 may enhance the preservation of morphological features while decay can stimulate mineral
575 replacement (e.g., pyritization, phosphatization) and/or the encapsulation of soft-tissues (e.g.,
576 concretion formation). Furthermore, H_2S-rich (euxinic) environments sustained by SRBs have
577 been shown to mediate the preservation of organic compounds via macromolecular incorporation
578 and reduction (Adam et al., 2000; Hebting, 2006; Melendez et al., 2013b).
579 Biomarker results indicate SRB may have been responsible for concretions at Greenland
580 and Canada as branched-chain fatty acids ($brC_{17:0}$) (Figure 5) and an unusual n-alkane C_{max} (C_{18})
581 (Figure 3b) were detected. However, two key differences between locations are the detection of
582 endogenous capelin tissue and significant algal lipids in Greenland (Figure 6, Table 2). This is
583 important because biomarker results from Greenland illustrate a highly productive water column
584 fed by glacier-induced mass wasting resulting in massive organic matter input into fjord bottom
585 waters. In particular, bacterial sulfate-reduction has been shown to be directly proportional to

This article is protected by copyright. All rights reserved

organic matter input not sulfate availability (Edenborn et al., 1987; Jørgensen et al., 1982). A key implication is that bottom waters at Kangerlussuaq fjord likely sustained a considerable bicarbonate (HCO_3^-) reservoir from enhanced SRB activity (Berner, 1968b). Then, as capelin mortality events occurred due to spawning, depositional conditions were conducive toward rapid carbonate encapsulation (Berner, 1968a). In contrast, biomarker results from Canada appear more consistent with relatively unproductive waters and negligeable organic matter input from the environment. Therefore, capelin decay may have directly contributed toward concretionary growth in lieu of an environmental bicarbonate reservoir (Berner, 1968a).

Although biomarker results indicate the presence of SRB at both sites, we are unable to ascribe preservation differences observed between sites to Hypothesis I. First, the presence of SRB shows no relationship to capelin soft-tissue preservation (Figure 6). CFL samples are most influenced by bacterial and environmental lipids in PC1 (Figure 6a), GFL samples are most influenced by algal lipids in PC2 (Figure 6a), and GFL samples are influenced by a mixture of algal lipids and capelin soft-tissue in PC3 (Figure 6b). Second, reduction and sulfurization of lipids do not appear to be key abiotic processes contributing to increased preservation at Greenland due to readily extractable and labile lipids in both free and carbonate-bound fractions (e.g., MUFAs, PUFAs, sterols, etc.). In particular, because sulfate reduction in marine environments is regulated by organic matter input, SRB activity at Kangerlussuaq may have been key toward sustaining particular porewater chemistries rather than enabling indirect abiotic preservation mechanisms. Hypothesis II therefore represents a viable proposition which emphasizes the depositional context (i.e., primary productivity, organic matter input, etc.) on the rate of concretion formation. In support of this, taphonomic experiments and statistical analysis of environmental parameters (i.e., host lithology, mineral composition, water chemistry, etc.) have emphasized the role of authigenic precipitation on exceptional preservation (Allison, 1988b; Briggs, 2003; McCoy et al., 2015b, 2015a; Sagemann et al., 1999). As microbial decay induces carbonate precipitation within shallow sediments, cementing pore spaces impede electron acceptor flow (e.g., SO_4^{2-}) into the decay foci resulting in attenuated microbial respiration (McCoy et al., 2015a, 2015b). Thus, it is important to understand how environmental parameters such as organic matter delivery, primary productivity, microbial respiration rates, sedimentation rate, and lithology could conceivably affect the post-depositional setting and influence concretion formation.

This article is protected by copyright. All rights reserved

4.6. Concretion formation at Greenland and Canada

Studies on concretion formation have generally noted that if porewaters are adequately supersaturated (i.e., SI > 0.8, Kempe and Kazmierczak, 1994), unremarkable bodies can act as simple nucleators (e.g., detritus, shells) for carbonate precipitation (Coleman and Raiswell, 1995; Pye et al., 1990; Raiswell, 1976). Conversely, in other environments, decaying organism may become the primary source of alkalinity driving precipitation (Coleman, 1993; Coleman and Raiswell, 1995; Raiswell, 1976). Early work by Berner, 1968a hypothesized that in supersaturated porewaters (i.e., 10 ppm $CaCO_3$), the rate of concretion growth may be modeled as a function of porewater velocity. That is, carbonate precipitation rates in stagnant post-depositional settings are diffusion limited and slow, meanwhile, precipitation rates in non-diffusion limited sediments are much faster. Work by Desaulniers and Cherry, 1989 has shown that sediments in the Ottawa Valley immediately adjacent to Greens Creek are composed of marine clays with measured porewater velocities (i.e., 2 meters/year) on-par with (modeled) stagnant, diffusion-limited, concretion formation (Berner, 1968a). On the other hand, while velocities are not available from Kangerlussuaq, measurements of analogous glacial deposits from Norwegian fjords estimate an excess of 100 meters/year (Soldal et al., 1994; Soldal and Rye, 1995). These observations suggest organic matter input, decay rates, and post-depositional properties are parameters which greatly influence the rate of concretion formation.

Modeled precipitations rates outlined in Berner, 1968a predict the Kangerlussuaq concretion (concretion radius = 1.5 cm, porewater velocity = 100 m/yr) could have formed within ~400 years and Greens Creek (concretion radius = 1.4 cm, porewater velocity = 2 m/yr) within ~1000 years. Accordingly, preliminary radiocarbon measurements across concretion transects reflect concentric growth patterns, out-to-in, which occurred within 450-years for Greenland and 1100-years for Canada (Mojarro et al., 2021). However, further investigation is required to confirm age trends and exclude possible mixing signals of old and young carbon that might introduce artefacts. Still, key implications are that: 1) low-permeability clays at Greens Creek may have impeded porewater circulation leading to decreased precipitation rates and persistent decay by SRB (and subsequently by other microbes as SO_4^{2-} became scarce) resulting in the complete remineralization of capelin tissues; 2) high-permeability sandy sediments supplemented by likely supersaturated carbonate porewaters (as indicated by organic matter

This article is protected by copyright. All rights reserved

input) at Kangerlussuaq facilitated rapid concretion formation. Given lipid analysis, modeling work, and known depositional parameters, we conclude preservation differences observed between Canada and Greenland represent varying rates of concretion formation (i.e., Hypothesis II).

5. Conclusions

Fish are commonly found in concretions, but the very recent occurrence of the same taxon (capelin) in different depositional environments has offered a unique opportunity to explore processes resulting in soft-tissue preservation. Here we have presented a comparative biomarker analysis of Holocene-age concretions from two environments that have produced highly contrasting fossils. 1) Kangerlussuaq, Greenland: a marine environment with recently exposed sediments due to isostatic rebound, and 2) Greens Creek, Ottawa, Canada: a paleo brackish-to-freshwater marine episode that resulted from the retreat of the Laurentide ice sheet. Given lipid biomarker evidence, we have determined that eutrophic conditions mediated enhanced rates of sedimentary sulfate-reduction resulting in porewater carbonate supersaturation at Kangerlussuaq. Porous sandy sediments then permitted rapid porewater velocities (e.g., non-diffusion-limited) resulting in a subsequent increase of carbonate precipitation rates accounting for soft-tissue preservation. We propose that exceptional preservation within concretions possibly occurs via the following steps and, in its simplest iteration, represents a race between precipitation and decay: 1) organic matter input feeds heterotrophic microbial communities sustaining large carbonate reservoirs, 2) high porewater velocities replenish ions (e.g., HCO_3^-, Fe^{2+}, Ca^{2+}, etc.) spent at sites of active precipitation, and 3) decay decreases (and ultimately ceases) in response to a cementing pore spaces. It remains unknown whether Greens Creek concretions were the sole byproducts of SRB or a microbial consortium of sulfate-reducers, iron-reducers, or methanogens (for instance) because of predicted seasonal limitation of SO_4^{2-}. If so, microbes using lower-efficiency redox couples did not necessarily yield an increased preservation potential at Greens Creek. Lastly, while the role of H_2S was not explicitly involved with enhanced biomarker preservation at Kangerlussuaq, Raney nickel desulfurization experiments confirmed the presence of a recalcitrant sulfurized macromolecular fraction which have been observed to persist over geological timescales.

This article is protected by copyright. All rights reserved

Author Disclosure Statement

No competing financial interests exist.

References

Ackman, R.G., Tocher, C.S., McLachlan, J., 1968. Marine Phytoplankter Fatty Acids. Journal of the Fisheries Board of Canada. https://doi.org/10.1139/f68-145

Adam, P., Schneckenburger, P., Schaeffer, P., Albrecht, P., 2000. Clues to early diagenetic sulfurization processes from mild chemical cleavage of labile sulfur-rich geomacromolecules. Geochimica et Cosmochimica Acta 64, 3485–3503. https://doi.org/10.1016/S0016-7037(00)00443-9

Alleon, J., Bernard, S., Le Guillou, C., Daval, D., Skouri-Panet, F., Kuga, M., Robert, F., 2017. Organic molecular heterogeneities can withstand diagenesis. Sci Rep 7, 1508. https://doi.org/10.1038/s41598-017-01612-8

Allison, P.A., 1988a. Konservat-Lagerstatten: cause and classification. Paleobiology 14, 331–344. https://doi.org/10.1017/S0094837300012082

Allison, P.A., 1988b. The role of anoxia in the decay and mineralization of proteinaceous macro-fossils. Paleobiology 14, 139–154. https://doi.org/10.1017/S009483730001188X

Allison, P.A., 1986. Soft-bodied animals in the fossil record: The role of decay in fragmentation during transport. Geology 14, 979–981.

Aloulou, F., Kallel, M., Dammak, M., Elleuch, B., Saliot, A., 2010. Even-numbered n-alkanes/n-alkenes predominance in surface sediments of Gabes Gulf in Tunisia. Environ Earth Sci 61, 1–10. https://doi.org/10.1007/s12665-009-0315-y

Andersen F (1996) Fate of organic carbon added as diatom cells to oxic and anoxic marine sediment microcosms. Marine Ecology Progress Series 134, 225–233.

Mojarro, A., Uveges, B. Roberts, M., Vinther, J., Summons, R.E. (2021) Preliminary ams 14C measurements from holocene-age carbonate concretions. In: 30th International Meeting on Organic Geochemistry. European Association of Geoscientists & Engineers, pp. 1–2. https://doi.org/10.3997/2214-4609.202134227

Bennike, O., 1997. Quaternary vertebrates from Greenland: A review. Quaternary Science Reviews 16, 899–909. https://doi.org/10.1016/S0277-3791(97)00002-4

This article is protected by copyright. All rights reserved

709 Berner, R. A., 1968a. Rate of concretion growth. Geochimica et Cosmochimica Acta 32, 477–
710 483. https://doi.org/10.1016/0016-7037(68)90040-9
711 Berner, R.A., 1969. Chemical changes affecting dissolved calcium during the bacterial
712 decomposition of fish and clams in sea water. Marine Geology 7, 253–274.
713 https://doi.org/10.1016/0025-3227(69)90011-5
714 Berner, R.A., 1968b. Calcium Carbonate Concretions Formed by the Decomposition of Organic
715 Matter. Science 159, 195–197. https://doi.org/10.1126/science.159.3811.195
716 Berner, R.A., Scott, M.R., Thomlinson, C., 1970. Carbonate alkalinity in the pore waters of
717 anoxic marine sediments1: carbonate alkalinity in sediment pore waters. Limnol.
718 Oceanogr. 15, 544–549. https://doi.org/10.4319/lo.1970.15.4.0544
719 Bianchi, T.S., Canuel, E.A., 2011. Chemical biomarkers in aquatic ecosystems. Princeton
720 University Press, Princeton.
721 Blumenberg, M., Thiel, V., Reitner, J., 2015. Organic matter preservation in the carbonate matrix
722 of a recent microbial mat – Is there a 'mat seal effect'? Organic Geochemistry 87, 25–34.
723 https://doi.org/10.1016/j.orggeochem.2015.07.005
724 Bray, E.E., Evans, E.D., 1961. Distribution of n-paraffins as a clue to recognition of source beds.
725 Geochimica et Cosmochimica Acta 22, 2–15. https://doi.org/10.1016/0016-
726 7037(61)90069-2
727 Briggs, D.E.G., 2003. The Role of Decay and Mineralization in the Preservation of Soft-Bodied
728 Fossils. Annual Review of Earth and Planetary Sciences 31, 275–301.
729 https://doi.org/10.1146/annurev.earth.31.100901.144746
730 Briggs, D.E.G., 1995. Experimental Taphonomy. PALAIOS 10, 539–550.
731 https://doi.org/10.2307/3515093
732 Briggs, D.E.G., Kear, A.J., 1993. Decay and preservation of polychaetes: taphonomic thresholds
733 in soft-bodied organisms. Paleobiology 19, 107–135.
734 https://doi.org/10.1017/S0094837300012343
735 Briggs, D.E.G., McMahon, S., 2016. The role of experiments in investigating the taphonomy of
736 exceptional preservation. Palaeontology 59, 1–11. https://doi.org/10.1111/pala.12219
737 Briggs, D.E.G., Summons, R.E., 2014. Ancient biomolecules: Their origins, fossilization, and
738 role in revealing the history of life: Prospects & Overviews. BioEssays 36, 482–490.
739 https://doi.org/10.1002/bies.201400010

This article is protected by copyright. All rights reserved

740 Brink, N.W. ten, 1975. Holocene history of the Greenland ice sheet based on radiocarbon-dated
741 moraines in West Greenland, Meddelelser om Gronland ; bd. 201, nr. 4. Kommissionen
742 for Videnskabelige Undersogelser : C. A. Reitzel, Kobenhavn.
743 Brown, C.M., Henderson, D.M., Vinther, J., Fletcher, I., Sistiaga, A., Herrera, J., Summons,
744 R.E., 2017. An Exceptionally Preserved Three-Dimensional Armored Dinosaur Reveals
745 Insights into Coloration and Cretaceous Predator-Prey Dynamics. Current Biology 27,
746 2514-2521.e3. https://doi.org/10.1016/j.cub.2017.06.071
747 Butler, A.D., Cunningham, J.A., Budd, G.E., Donoghue, P.C.J., 2015. Experimental taphonomy
748 of Artemia reveals the role of endogenous microbes in mediating decay and fossilization.
749 Proc. R. Soc. B. 282, 20150476. https://doi.org/10.1098/rspb.2015.0476
750 Clements, T., Purnell, M., Gabbott, S., 2019. The Mazon Creek Lagerstätte: a diverse late
751 Paleozoic ecosystem entombed within siderite concretions. Journal of the Geological
752 Society 176, 1–11. https://doi.org/10.1144/jgs2018-088
753 Coleman, M.L., 1993. Microbial processes: Controls on the shape and composition of carbonate
754 concretions. Marine Geology 113, 127–140. https://doi.org/10.1016/0025-
755 3227(93)90154-N
756 Coleman, M.L., Raiswell, R., 1995. Source of carbonate and origin of zonation in pyritiferous
757 carbonate concretions; evaluation of a dynamic model. Am J Sci 295, 282–308.
758 https://doi.org/10.2475/ajs.295.3.282
759 Coleman, M.L., Raiswell, R., 1981. Carbon, oxygen and sulphur isotope variations in
760 concretions from the Upper Lias of N.E. England. Geochimica et Cosmochimica Acta 45,
761 329–340. https://doi.org/10.1016/0016-7037(81)90243-X
762 Crisp, M., Demarchi, B., Collins, M., Morgan-Williams, M., Pilgrim, E., Penkman, K., 2013.
763 Isolation of the intra-crystalline proteins and kinetic studies in Struthio camelus (ostrich)
764 eggshell for amino acid geochronology. Quaternary Geochronology 16, 110–128.
765 https://doi.org/10.1016/j.quageo.2012.09.002
766 Cronin, T.M., Manley, P.L., Brachfeld, S., Manley, T.O., Willard, D.A., Guilbault, J.-P.,
767 Rayburn, J.A., Thunell, R., Berke, M., 2008. Impacts of post-glacial lake drainage events
768 and revised chronology of the Champlain Sea episode 13–9 ka. Palaeogeography,
769 Palaeoclimatology, Palaeoecology 262, 46–60.
770 https://doi.org/10.1016/j.palaeo.2008.02.001

This article is protected by copyright. All rights reserved

771 Darroch, S.A.F., Laflamme, M., Schiffbauer, J.D., Briggs, D.E.G., 2012. Experimental formation
772 of a microbial death mask. PALAIOS 27, 293–303.
773 https://doi.org/10.2110/palo.2011.p11-059r
774 Davis, J.B., 1968. Paraffinic hydrocarbons in the sulfate-reducing bacterium Desulfovibrio
775 desulfuricans. Chemical Geology 3, 155–160. https://doi.org/10.1016/0009-
776 2541(68)90007-7
777 Demarchi, B., Hall, S., Roncal-Herrero, T., Freeman, C.L., Woolley, J., Crisp, M.K., Wilson, J.,
778 Fotakis, A., Fischer, R., Kessler, B.M., Rakownikow Jersie-Christensen, R., Olsen, J.V.,
779 Haile, J., Thomas, J., Marean, C.W., Parkington, J., Presslee, S., Lee-Thorp, J.,
780 Ditchfield, P., Hamilton, J.F., Ward, M.W., Wang, C.M., Shaw, M.D., Harrison, T.,
781 Domínguez-Rodrigo, M., MacPhee, R.D., Kwekason, A., Ecker, M., Kolska Horwitz, L.,
782 Chazan, M., Kröger, R., Thomas-Oates, J., Harding, J.H., Cappellini, E., Penkman, K.,
783 Collins, M.J., 2016. Protein sequences bound to mineral surfaces persist into deep time.
784 eLife 5, e17092. https://doi.org/10.7554/eLife.17092
785 Desaulniers, D.E., Cherry, J.A., 1989a. Origin and movement of groundwater and major ions in a
786 thick deposit of Champlain Sea clay near Montréal. Can. Geotech. J. 26, 80–89.
787 https://doi.org/10.1139/t89-009
788 Desaulniers, D.E., Cherry, J.A., 1989b. Origin and movement of groundwater and major ions in
789 a thick deposit of Champlain Sea clay near Montréal. Can. Geotech. J. 26, 80–89.
790 https://doi.org/10.1139/t89-009
791 Dietrich, R., Rülke, A., Scheinert, M., 2005. Present-day vertical crustal deformations in West
792 Greenland from repeated GPS observations. Geophys J Int 163, 865–874.
793 https://doi.org/10.1111/j.1365-246X.2005.02766.x
794 Dowling, N.J.E., Widdel, F., White, D.C., 1986. Phospholipid Ester-linked Fatty Acid
795 Biomarkers of Acetate-oxidizing Sulphate-reducers and Other Sulphide-forming
796 Bacteria. Microbiology, 132, 1815–1825. https://doi.org/10.1099/00221287-132-7-1815
797 Drenzek, N.J., Montluçon, D.B., Yunker, M.B., Macdonald, R.W., Eglinton, T.I., 2007.
798 Constraints on the origin of sedimentary organic carbon in the Beaufort Sea from coupled
799 molecular 13C and 14C measurements. Marine Chemistry 103, 146–162.
800 https://doi.org/10.1016/j.marchem.2006.06.017

This article is protected by copyright. All rights reserved

801 Duan, W.M., Hedrick, D.B., Pye, K., Coleman, hf. L., White, D.C., 1996. A preliminary study
802 of the geochemical and microbiological characteristics of modern sedimentary
803 concretions. Limnol. Oceanogr. 41, 1404–1414.
804 https://doi.org/10.4319/lo.1996.41.7.1404
805 Dupraz, C., Reid, R.P., Braissant, O., Decho, A.W., Norman, R.S., Visscher, P.T., 2009.
806 Processes of carbonate precipitation in modern microbial mats. Earth-Science Reviews
807 96, 141–162. https://doi.org/10.1016/j.earscirev.2008.10.005
808 Edenborn, H.M., Silverberg, N., Mucci, A., Sundby, B., 1987. Sulfate reduction in deep coastal
809 marine sediments. Marine Chemistry 21, 329–345. https://doi.org/10.1016/0304-
810 4203(87)90055-7
811 Eglinton, G., Hamilton, R.J., 1967. Leaf Epicuticular Waxes. Science 156, 1322–1335.
812 https://doi.org/10.1126/science.156.3780.1322
813 Elder, R.L., Smith, G.R., 1988. Fish taphonomy and environmental inference in paleolimnology.
814 Palaeogeography, Palaeoclimatology, Palaeoecology 62, 577–592.
815 https://doi.org/10.1016/0031-0182(88)90072-7
816 Elvert, M., Boetius, A., Knittel, K., Jørgensen, B.B., 2003. Characterization of Specific
817 Membrane Fatty Acids as Chemotaxonomic Markers for Sulfate-Reducing Bacteria
818 Involved in Anaerobic Oxidation of Methane. Geomicrobiology Journal 20, 403–419.
819 https://doi.org/10.1080/01490450303894
820 Fabbri, M., Wiemann, J., Manucci, F., Briggs, D.E.G., 2020. Three-dimensional soft tissue
821 preservation revealed in the skin of a non-avian dinosaur. Palaeontology 63, 185–193.
822 https://doi.org/10.1111/pala.12470
823 Gäb, F., Ballhaus, C., Stinnesbeck, E., Kral, A.G., Janssen, K., Bierbaum, G., 2020.
824 Experimental taphonomy of fish - role of elevated pressure, salinity and pH. Sci Rep 10,
825 7839. https://doi.org/10.1038/s41598-020-64651-8
826 Gadd, N.R., 1980. Maximum age for a concretion at Green Creek, Ontario. Géographie physique
827 et Quaternaire 34, 229. https://doi.org/10.7202/1000400ar
828 Gaines, R.R., Kennedy, M.J., Droser, M.L., 2005. A new hypothesis for organic preservation of
829 Burgess Shale taxa in the middle Cambrian Wheeler Formation, House Range, Utah.
830 Palaeogeography, Palaeoclimatology, Palaeoecology, Interpretation of Biological and

This article is protected by copyright. All rights reserved

Environmental Changes across the Neoproterozoic-Cambrian Boundary 220, 193–205. https://doi.org/10.1016/j.palaeo.2004.07.034

Grice, K., Holman, A.I., Plet, C., Tripp, M., 2019. Fossilised Biomolecules and Biomarkers in Carbonate Concretions from Konservat-Lagerstätten. Minerals 9, 158. https://doi.org/10.3390/min9030158

Grimalt, J., Albaigés, J., 1987. Sources and occurrence of C12□C22n-alkane distributions with even carbon-number preference in sedimentary environments. Geochimica et Cosmochimica Acta 51, 1379–1384. https://doi.org/10.1016/0016-7037(87)90322-X

Gupta, N.S., Cody, G.D., Tetlie, O.E., Briggs, D.E.G., Summons, R.E., 2009. Rapid incorporation of lipids into macromolecules during experimental decay of invertebrates: Initiation of geopolymer formation. Organic Geochemistry 40, 589–594. https://doi.org/10.1016/j.orggeochem.2009.02.005

Han, J., Calvin, M., 1969. Hydrocarbon Distribution of Algae and Bacteria, and Microbiological Activity in Sediments. PNAS 64, 436–443. https://doi.org/10.1073/pnas.64.2.436

Hebting, Y., 2006. Biomarker Evidence for a Major Preservation Pathway of Sedimentary Organic Carbon. Science 312, 1627–1631. https://doi.org/10.1126/science.1126372

Hedges, J.I., Keil, R.G., 1995. Sedimentary organic matter preservation: an assessment and speculative synthesis. Marine Chemistry 49, 81–115. https://doi.org/10.1016/0304-4203(95)00008-F

Henkemans, E., Frape, S.K., Ruskeeniemi, T., Anderson, N.J., Hobbs, M., 2018. A landscape-isotopic approach to the geochemical characterization of lakes in the Kangerlussuaq region, west Greenland. Arctic, Antarctic, and Alpine Research 50, S100018. https://doi.org/10.1080/15230430.2017.1420863

Hinrichs, K.-U., Summons, R.E., Orphan, V., Sylva, S.P., Hayes, J.M., 2000. Molecular and isotopic analysis of anaerobic methane-oxidizing communities in marine sediments. Organic Geochemistry 31, 1685–1701. https://doi.org/10.1016/S0146-6380(00)00106-6

Holman, J.A., Harington, C.R., Mott, R.J., 1997. Skeleton of a leopard frog (Rana pipiens) from Champlain Sea deposits (ca. 10,000 BP) near Eardley, Quebec. Can. J. Earth Sci. 34, 1150–1155. https://doi.org/10.1139/e17-092

Hotelling, H., 1933. Analysis of a complex of statistical variables into principal components. Journal of educational psychology 24, 417.

This article is protected by copyright. All rights reserved

862 Ingalls, A.E., Aller, R.C., Lee, C., Wakeham, S.G., 2004. Organic matter diagenesis in shallow
863 water carbonate sediments. Geochimica et Cosmochimica Acta 68, 4363–4379.
864 https://doi.org/10.1016/j.gca.2004.01.002
865 Iniesto, M., Laguna, C., Florín, M., Guerrero, M.C., Chicote, A., Buscalioni, A.D., López-
866 Archilla, A.I., 2015. The impact of microbial mats and their microenvironmental
867 conditions in early decay of fish. PALAIOS 30, 792–801.
868 https://doi.org/10.2110/palo.2014.086
869 Iniesto, M., Lopez-Archilla, A.I., Fregenal-Martinez, M., Buscalioni, A.D., Guerrero, M.C.,
870 2013. Involvement of microbial mats in delayed decay: an experimental essay on fish
871 preservation. PALAIOS 28, 56–66. https://doi.org/10.2110/palo.2011.p11-099r
872 Iniesto, M., Villalba, I., Buscalioni, A.D., Guerrero, M.C., López-Archilla, A.I., 2017. The Effect
873 Of microbial Mats In The Decay Of Anurans With Implications For Understanding
874 Taphonomic Processes In The Fossil Record. Sci Rep 7, 45160.
875 https://doi.org/10.1038/srep45160
876 Jørgensen, B.B., Postgate, J.R., Postgate, J.R., Kelly, D.P., 1982. Ecology of the bacteria of the
877 sulphur cycle with special reference to anoxic—oxic interface environments.
878 Philosophical Transactions of the Royal Society of London. B, Biological Sciences 298,
879 543–561. https://doi.org/10.1098/rstb.1982.0096
880 Kempe, S., Kazmierczak, J., 1994. The role of alkalinity in the evolution of ocean chemistry,
881 organization of living systems, and biocalcification processes. Bulletin de la Institut
882 Océanographique (Monaco) 13, 61–117.
883 Larter, S.R., Douglas, A.G., 1980. Melanoidins—kerogen precursors and geochemical lipid
884 sinks: a study using pyrolysis gas chromatography (PGC). Geochimica et Cosmochimica
885 Acta 44, 2087–2095. https://doi.org/10.1016/0016-7037(80)90206-9
886 Lehmann MF, Bernasconi SM, Barbieri A, McKenzie JA (2002) Preservation of organic matter
887 and alteration of its carbon and nitrogen isotope composition during simulated and in situ
888 early sedimentary diagenesis. Geochimica et Cosmochimica Acta 66, 3573–3584.
889 Lengger, S.K., Melendez, I.M., Summons, R.E., Grice, K., 2017. Mudstones and embedded
890 concretions show differences in lithology-related, but not source-related biomarker
891 distributions. Organic Geochemistry 113, 67–74.
892 https://doi.org/10.1016/j.orggeochem.2017.08.003

This article is protected by copyright. All rights reserved

893 Lindgren, J., Uvdal, P., Sjövall, P., Nilsson, D.E., Engdahl, A., Schultz, B.P., Thiel, V., 2012.
894 Molecular preservation of the pigment melanin in fossil melanosomes. Nature
895 Communications 3, 824. https://doi.org/10.1038/ncomms1819
896 McAllister, D.E., Cumbaa, S.L., Harington, C.R., 1981. Pleistocene fishes (Coregonus, Osmerus,
897 Microgadus, Gasterosteus) from Green Creek, Ontario, Canada. Canadian Journal of
898 Earth Sciences 18, 1356–1364. https://doi.org/10.1139/e81-125
899 Mcbride, E.F., Milliken, K.L., 2006. Giant calcite-cemented concretions, Dakota Formation,
900 central Kansas, USA: Giant concretions in Dakota Sandstone, Kansas, USA.
901 Sedimentology 53, 1161–1179. https://doi.org/10.1111/j.1365-3091.2006.00813.x
902 McCoy, V.E., Wiemann, J., Lamsdell, J.C., Whalen, C.D., Lidgard, S., Mayer, P., Petermann,
903 H., Briggs, D.E.G., 2020. Chemical signatures of soft tissues distinguish between
904 vertebrates and invertebrates from the Carboniferous Mazon Creek Lagerstätte of Illinois.
905 Geobiology 18, 560–565. https://doi.org/10.1111/gbi.12397
906 McCoy, V.E., Young, R.T., Briggs, D.E.G., 2015a. Sediment permeability and the preservation
907 of soft-tissues in concretions: an experimental study. PALAIOS 30, 608–612.
908 https://doi.org/10.2110/palo.2015.002
909 McCoy, V.E., Young, R.T., Briggs, D.E.G., 2015b. Factors controlling exceptional preservation
910 in concretions. PALAIOS 30, 272–280. https://doi.org/10.2110/palo.2014.081
911 McKirdy, D.M., Thorpe, C.S., Haynes, D.E., Grice, K., Krull, E.S., Halverson, G.P., Webster,
912 L.J., 2010. The biogeochemical evolution of the Coorong during the mid- to late
913 Holocene: An elemental, isotopic and biomarker perspective. Organic Geochemistry,
914 2008 Australian Organic Geochemistry Conference: A national conference held in
915 association with the International Humic Substances Society and the Natural Organic
916 Matter Interest Group 41, 96–110. https://doi.org/10.1016/j.orggeochem.2009.07.010
917 Mcnamara, M.E., Orr, P.J., Kearns, S.L., Alcala, L., Anadon, P., Penalver Molla, E., 2009. Soft-
918 tissue preservation in miocene frogs from libros, spain: insights into the genesis of decay
919 microenvironments. PALAIOS 24, 104–117. https://doi.org/10.2110/palo.2008.p08-017r
920 Melendez, I., Grice, K., Schwark, L., 2013a. Exceptional preservation of Palaeozoic steroids in a
921 diagenetic continuum. Scientific Reports 3. https://doi.org/10.1038/srep02768
922 Melendez, I., Grice, K., Trinajstic, K., Ladjavardi, M., Greenwood, P., Thompson, K., 2013b.
923 Biomarkers reveal the role of photic zone euxinia in exceptional fossil preservation: An

This article is protected by copyright. All rights reserved

organic geochemical perspective. Geology 41, 123–126. https://doi.org/10.1130/G33492.1

Meyers, P.A., 1997. Organic geochemical proxies of paleoceanographic, paleolimnologic, and paleoclimatic processes. Organic Geochemistry 27, 213–250. https://doi.org/10.1016/S0146-6380(97)00049-1

Mozley, P.S., 1996. The internal structure of carbonate concretions in mudrocks: a critical evaluation of the conventional concentric model of concretion growth. Sedimentary Geology 103, 85–91. https://doi.org/10.1016/0037-0738(95)00087-9

Muscente, A.D., Schiffbauer, J.D., Broce, J., Laflamme, M., O'Donnell, K., Boag, T.H., Meyer, M., Hawkins, A.D., Huntley, J.W., McNamara, M., MacKenzie, L.A., Stanley, G.D., Hinman, N.W., Hofmann, M.H., Xiao, S., 2017. Exceptionally preserved fossil assemblages through geologic time and space. Gondwana Research 48, 164–188. https://doi.org/10.1016/j.gr.2017.04.020

Naimark, E., Kalinina, M., Shokurov, A., Boeva, N., Markov, A., Zaytseva, L., 2016. Decaying in different clays: implications for soft-tissue preservation. Palaeontology 59, 583–595. https://doi.org/10.1111/pala.12246

Nakashima, B., 2002. Capelin (Mallotus villosus) spawning behaviour in Newfoundland waters – the interaction between beach and demersal spawning. ICES Journal of Marine Science 59, 909–916. https://doi.org/10.1006/jmsc.2002.1261

Nishimura, M., Baker, E.W., 1986. Possible origin of n-alkanes with a remarkable even-to-odd predominance in recent marine sediments. Geochimica et Cosmochimica Acta 50, 299–305. https://doi.org/10.1016/0016-7037(86)90178-X

O'Reilly, S.S., Mariotti, G., Winter, A.R., Newman, S.A., Matys, E.D., McDermott, F., Pruss, S.B., Bosak, T., Summons, R.E., Klepac-Ceraj, V., 2017. Molecular biosignatures reveal common benthic microbial sources of organic matter in ooids and grapestones from Pigeon Cay, The Bahamas. Geobiology 15, 112–130. https://doi.org/10.1111/gbi.12196

Oskam, C.L., Haile, J., McLay, E., Rigby, P., Allentoft, M.E., Olsen, M.E., Bengtsson, C., Miller, G.H., Schwenninger, J.-L., Jacomb, C., Walter, R., Baynes, A., Dortch, J., Parker-Pearson, M., Gilbert, M.T.P., Holdaway, R.N., Willerslev, E., Bunce, M., 2010. Fossil avian eggshell preserves ancient DNA. Proc. R. Soc. B 277, 1991–2000. https://doi.org/10.1098/rspb.2009.2019

This article is protected by copyright. All rights reserved

955 Parent, M., Occhietti, S., 1988. Late Wisconsinan Deglaciation and Champlain Sea Invasion in
956 the St. Lawrence Valley, Québec. Géographie physique et Quaternaire 42, 215.
957 https://doi.org/10.7202/032734ar
958 Parry, L.A., Smithwick, F., Nordén, K.K., Saitta, E.T., Lozano-Fernandez, J., Tanner, A.R.,
959 Caron, J.-B., Edgecombe, G.D., Briggs, D.E.G., Vinther, J., 2018. Soft-Bodied Fossils
960 Are Not Simply Rotten Carcasses - Toward a Holistic Understanding of Exceptional
961 Fossil Preservation: Exceptional Fossil Preservation Is Complex and Involves the
962 Interplay of Numerous Biological and Geological Processes. BioEssays 40, 1700167.
963 https://doi.org/10.1002/bies.201700167
964 Plet, C., Grice, K., Pagès, A., Verrall, M., Coolen, M.J.L., Ruebsam, W., Rickard, W.D.A.,
965 Schwark, L., 2017. Palaeobiology of red and white blood cell-like structures, collagen
966 and cholesterol in an ichthyosaur bone. Sci Rep 7, 13776. https://doi.org/10.1038/s41598-
967 017-13873-4
968 Prost, K., Birk, J.J., Lehndorff, E., Gerlach, R., Amelung, W., 2017. Steroid Biomarkers
969 Revisited – Improved Source Identification of Faecal Remains in Archaeological Soil
970 Material. PLoS ONE 12, e0164882. https://doi.org/10.1371/journal.pone.0164882
971 Purnell, M.A., Donoghue, P.J.C., Gabbott, S.E., McNamara, M.E., Murdock, D.J.E., Sansom,
972 R.S., 2018. Experimental analysis of soft-tissue fossilization: opening the black box.
973 Palaeontology 61, 317–323. https://doi.org/10.1111/pala.12360
974 Pye, K., Dickson, J.A.D., Schiavon, N., Coleman, M.L., Cox, M., 1990. Formation of siderite-
975 Mg-calcite-iron sulphide concretions in intertidal marsh and sandflat sediments, north
976 Norfolk, England. Sedimentology 37, 325–343. https://doi.org/10.1111/j.1365-
977 3091.1990.tb00962.x
978 Raiswell, R., 1976. The microbiological formation of carbonate concretions in the Upper Lias of
979 NE England. Chemical Geology 18, 227–244. https://doi.org/10.1016/0009-
980 2541(76)90006-1
981 Raiswell, R., Fisher, Q.J., 2000. Mudrock-hosted carbonate concretions: a review of growth
982 mechanisms and their influence on chemical and isotopic composition. Journal of the
983 Geological Society 157, 239–251. https://doi.org/10.1144/jgs.157.1.239
984 Ran-Ressler, R.R., Lawrence, P., Brenna, J.T., 2012. Structural characterization of saturated
985 branched chain fatty acid methyl esters by collisional dissociation of molecular ions

This article is protected by copyright. All rights reserved

generated by electron ionization. Journal of Lipid Research 53, 195–203. https://doi.org/10.1194/jlr.D020651

Řezanka, T., 1989. Very-long-chain fatty acids from the animal and plant kingdoms. Progress in Lipid Research 28, 147–187. https://doi.org/10.1016/0163-7827(89)90011-8

Řezanka T, Sokolov MY, Víden I (1990) Unusual and very-long-chain fatty acids in Desulfotomaculum, a sulfate-reducing bacterium. FEMS Microbiology Letters 73, 231-237.

Rielley, G., Collier, R.J., Jones, D.M., Eglinton, G., 1991. The biogeochemistry of Ellesmere Lake, U.K.—I: source correlation of leaf wax inputs to the sedimentary lipid record. Organic Geochemistry 17, 901–912. https://doi.org/10.1016/0146-6380(91)90031-E

Sagemann, J., Bale, S.J., Briggs, D.E.G., Parkes, R.J., 1999. Controls on the formation of authigenic minerals in association with decaying organic matter: an experimental approach. Geochimica et Cosmochimica Acta 63, 1083–1095. https://doi.org/10.1016/S0016-7037(99)00087-3

Sand, K.K., Pedersen, C.S., Sjöberg, S., Nielsen, J.W., Makovicky, E., Stipp, S.L.S., 2014. Biomineralization: Long-Term Effectiveness of Polysaccharides on the Growth and Dissolution of Calcite. Crystal Growth & Design 14, 5486–5494. https://doi.org/10.1021/cg5006743

Sansom, R.S., 2014. Experimental Decay of Soft Tissues. Paleontol. Soc. pap. 20, 259–274. https://doi.org/10.1017/S1089332600002886

Sansom, R.S., Gabbott, S.E., Purnell, M.A., 2011. Decay of vertebrate characters in hagfish and lamprey (Cyclostomata) and the implications for the vertebrate fossil record. Proc. R. Soc. B. 278, 1150–1157. https://doi.org/10.1098/rspb.2010.1641

Seilacher, A., 2001. Concretion morphologies reflecting diagenetic and epigenetic pathways. Sedimentary Geology 143, 41–57.

Sigurgisladóttir, S., Pálmadóttir, H., 1993. Fatty acid composition of thirty-five Icelandic fish species. Journal of the American Oil Chemists Society 70, 1081–1087. https://doi.org/10.1007/BF02632146

Sinninghe Damsté, J.S., Irene, W., Rijpstra, C., de Leeuw, J.W., Schenck, P.A., 1988. Origin of organic sulphur compounds and sulphur-containing high molecular weight substances in

This article is protected by copyright. All rights reserved

sediments and immature crude oils. Organic Geochemistry 13, 593–606. https://doi.org/10.1016/0146-6380(88)90079-4

Smittenberg, R.H., Pancost, R.D., Hopmans, E.C., Paetzel, M., Sinninghe Damsté, J.S., 2004. A 400-year record of environmental change in an euxinic fjord as revealed by the sedimentary biomarker record. Palaeogeography, Palaeoclimatology, Palaeoecology 202, 331–351. https://doi.org/10.1016/S0031-0182(03)00642-4

Soldal, O., Mauring, E., Halvorsen, E., Rye, N., 1994. Seawater intrusion and fresh groundwater hydraulics in fjord delta aquifers inferred from ground penetrating radar and resistivity profiles—Sunndalsøra and Esebotn, western Norway. Journal of applied geophysics 32, 305–319.

Soldal, O., Rye, N., 1995. Hydrogeology of a fjord delta aquifer, Sunndalsøra, Norway. Norsk Geologisk Tidsskrift 75, 169–178.

Storms, J.E.A., de Winter, I.L., Overeem, I., Drijkoningen, G.G., Lykke-Andersen, H., 2012. The Holocene sedimentary history of the Kangerlussuaq Fjord-valley fill, West Greenland. Quaternary Science Reviews 35, 29–50. https://doi.org/10.1016/j.quascirev.2011.12.014

Summons R.E., Bird L.R., Gillespie A.L., Pruss S.B., Roberts M. and Sessions A.L., 2013. Lipid biomarkers in ooids from different locations and ages: evidence for a common bacterial flora Geobiology 11, 420–436.

Sun M., Wakeham SG, Lee C (1997) Rates and mechanisms of fatty acid degradation in oxic and anoxic coastal marine sediments of Long Island Sound, New York, USA. Geochimica et Cosmochimica Acta 61, 341–355.

Taylor, J., Parkes, R.J., 1983. The Cellular Fatty Acids of the Sulphate-reducing Bacteria, Desulfobacter sp., Desulfobulbus sp. and Desulfovibrio desulfuricans. Microbiology, 129, 3303–3309. https://doi.org/10.1099/00221287-129-11-3303

Thiel, V., Hoppert, M., 2018. Fatty acids and other biomarkers in two Early Jurassic concretions and their immediate host rocks (Lias δ, Buttenheim clay pit, Bavaria, Germany). Organic Geochemistry 120, 42–55. https://doi.org/10.1016/j.orggeochem.2018.02.010

Volkman, J.K., 2006. Lipid Markers for Marine Organic Matter, in: Volkman, J.K. (Ed.), Marine Organic Matter: Biomarkers, Isotopes and DNA. Springer-Verlag, Berlin/Heidelberg, pp. 27–70. https://doi.org/10.1007/698_2_002

This article is protected by copyright. All rights reserved

Volkman, J.K., Barrett, S.M., Blackburn, S.I., Mansour, M.P., Sikes, E.L., Gelin, F., 1998. Microalgal biomarkers: A review of recent research developments. Organic Geochemistry 29, 1163–1179. https://doi.org/10.1016/S0146-6380(98)00062-X

Volkman, J.K., Johns, R.B., Gillan, F.T., Perry, G.J., Bavor, H.J., 1980. Microbial lipids of an intertidal sediment—I. Fatty acids and hydrocarbons. Geochimica et Cosmochimica Acta 44, 1133–1143. https://doi.org/10.1016/0016-7037(80)90067-8

Wakeham, S.G., 1989. Reduction of stenols to stanols in particulate matter at oxic–anoxic boundaries in sea water. Nature 342, 787–790. https://doi.org/10.1038/342787a0

Wiemann, J., Crawford, J.M., Briggs, D.E.G., 2020. Phylogenetic and physiological signals in metazoan fossil biomolecules. Sci. Adv. 6, eaba6883. https://doi.org/10.1126/sciadv.aba6883

Wiemann, J., Fabbri, M., Yang, T.-R., Stein, K., Sander, P.M., Norell, M.A., Briggs, D.E.G., 2018. Fossilization transforms vertebrate hard tissue proteins into N-heterocyclic polymers. Nat Commun 9, 4741. https://doi.org/10.1038/s41467-018-07013-3

Wilson, D., Brett, C., 2013. Concretions as sources of exceptional preservation, and decay as a source of concretions: examples from the middle devonian of new york. PALAIOS 28, 305–316. https://doi.org/10.2110/palo.2012.p12-086r

Zatoń, M., Marynowski, L., 2004. Konzentrat-Lagerstätte-type carbonate concretions from the uppermost Bajocian (Middle Jurassic) of the Częstochowa area, South-Cental Poland. Geological Quarterly 48, 339–350.

This article is protected by copyright. All rights reserved

Figure 1: Capelin concretions analyzed in this study. The Greenland concretion was collected south-west of the Kangerlussuaq airport (67°00'06.8"N 50°46'19.8"W) by L. Lawaetz while the Canadian concretion was collected from Greens Creek, Ottawa, Ontario (45°27'56.6"N 75°34'34.7"W) by the Geological Survey of Canada (GSC loc. 60327). (a) The Kangerlussuaq concretion does not include a head but otherwise displays exceptional soft-tissue preservation (e.g., organic film in stomach area, skin impressions, color banding), (b) the Ottawa concretion is fully articulated but lacks tissue impressions and stomach contents illustrating a greater degree of decay (each bar is 1 cm).

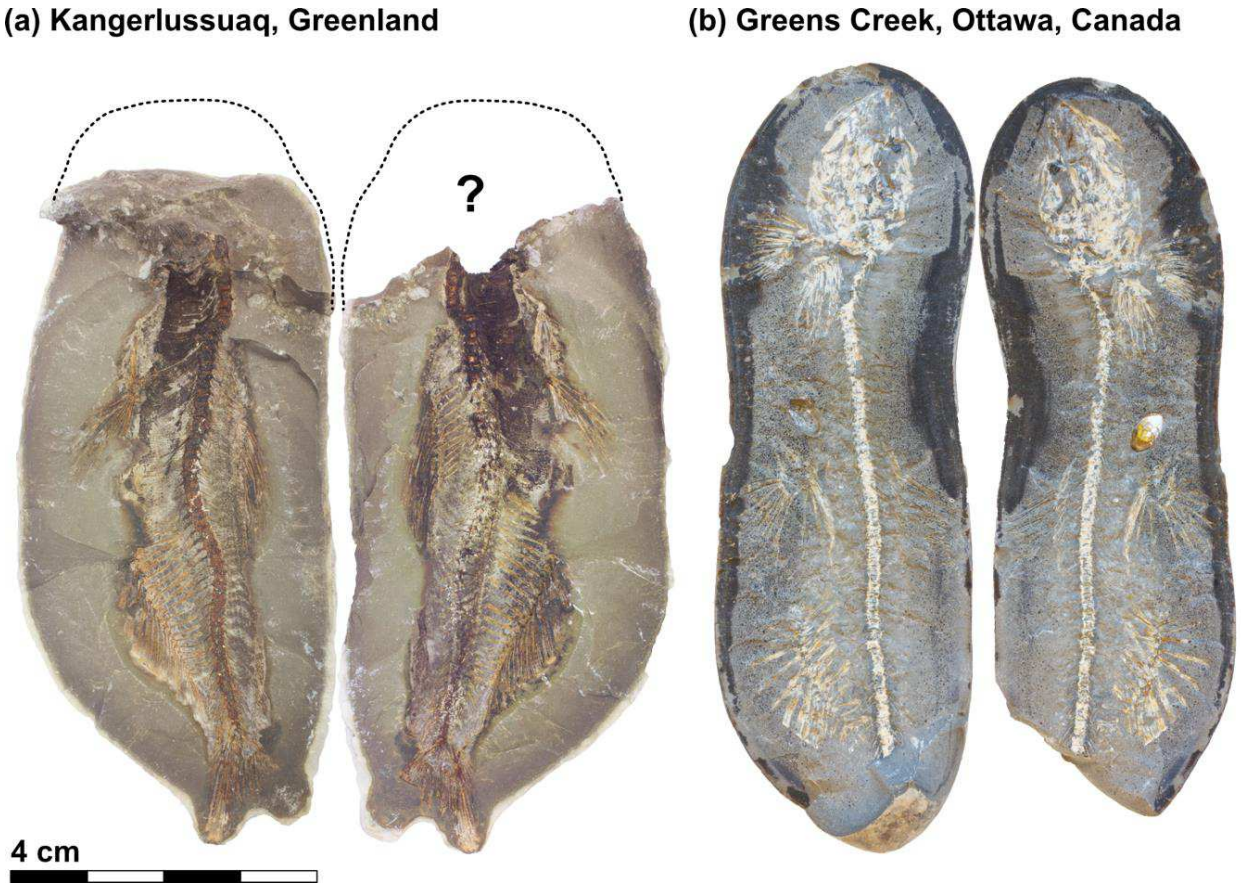

Figure 2: Sampling strategy. Approximately 10 mm of each concretion's exposed outer surface was removed via abrasion, ~2 mm thick slices oriented parallel to the fossil nucleus were then taken yielding 4 layers for each specimen (3D exaggeration not to scale). Results shown and

This article is protected by copyright. All rights reserved

discussed here are from the Greenland fossil layer* while results from Canada are from matrix 1^{+}.

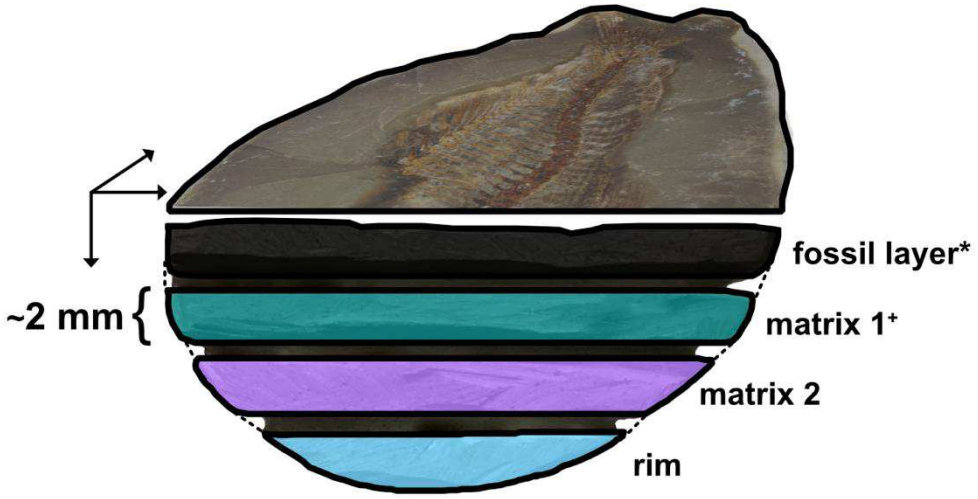

This article is protected by copyright. All rights reserved

Figure 3: Saturated hydrocarbons (F1). (a) Greenland free lipids display an odd-carbon preference for long-chain (C_{20} – C_{37}) n-alkanes with a C_{max} at C_{27} while (b) carbonate-bound lipids do not display a carbon preference with a C_{max} at C_{29}. (c) Canada free lipids display an unusual C_{max} at C_{18} while (d) carbonate-bound lipids (right y-axis) could only be detected via extracted ion chromatogram (EIC) of m/z 57 and do not display a carbon preference with a C_{max} at C_{29}.

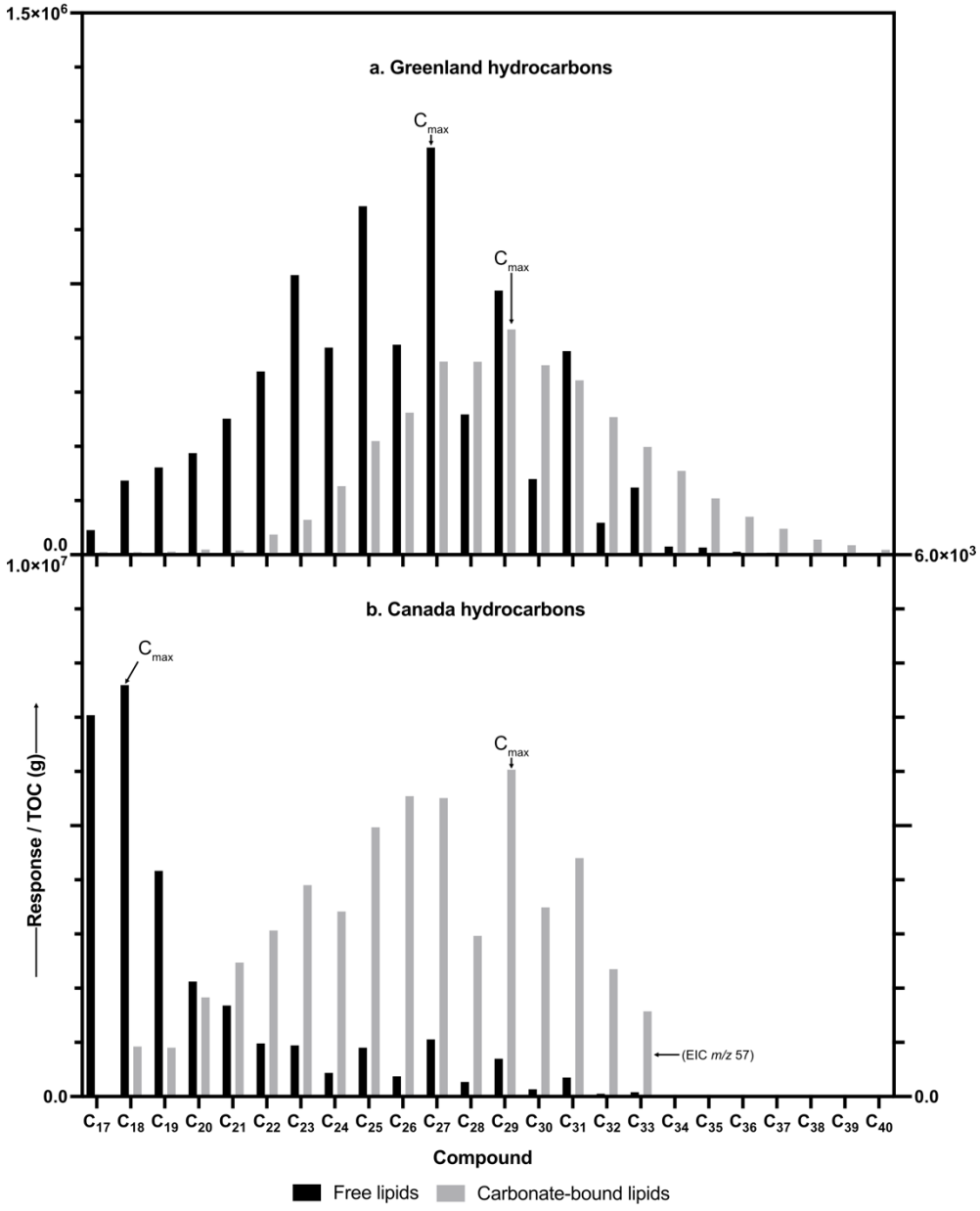

Figure 4: Biomarker ratios. (a) Pristane/phytane ratios indicate sustained reducing conditions in Greenland and possibly reducing-to-oxidizing at Canada. (b) Carbon preference index (CPI)

This article is protected by copyright. All rights reserved

generally demonstrate contrasting hydrocarbon maturities have been incorporated into the free lipid and carbonate fractions. (c) Terrigenous/aquatic ratios (TAR_{HC}) for n-alkanes demonstrate a higher terrestrial contribution in GFL, GCB, and CCB while CFL shows higher aquatic contributions. (d) Terrigenous/aquatic ratios (TAR_{FA}) for fatty acids show a greater aquatic contribution for all samples.

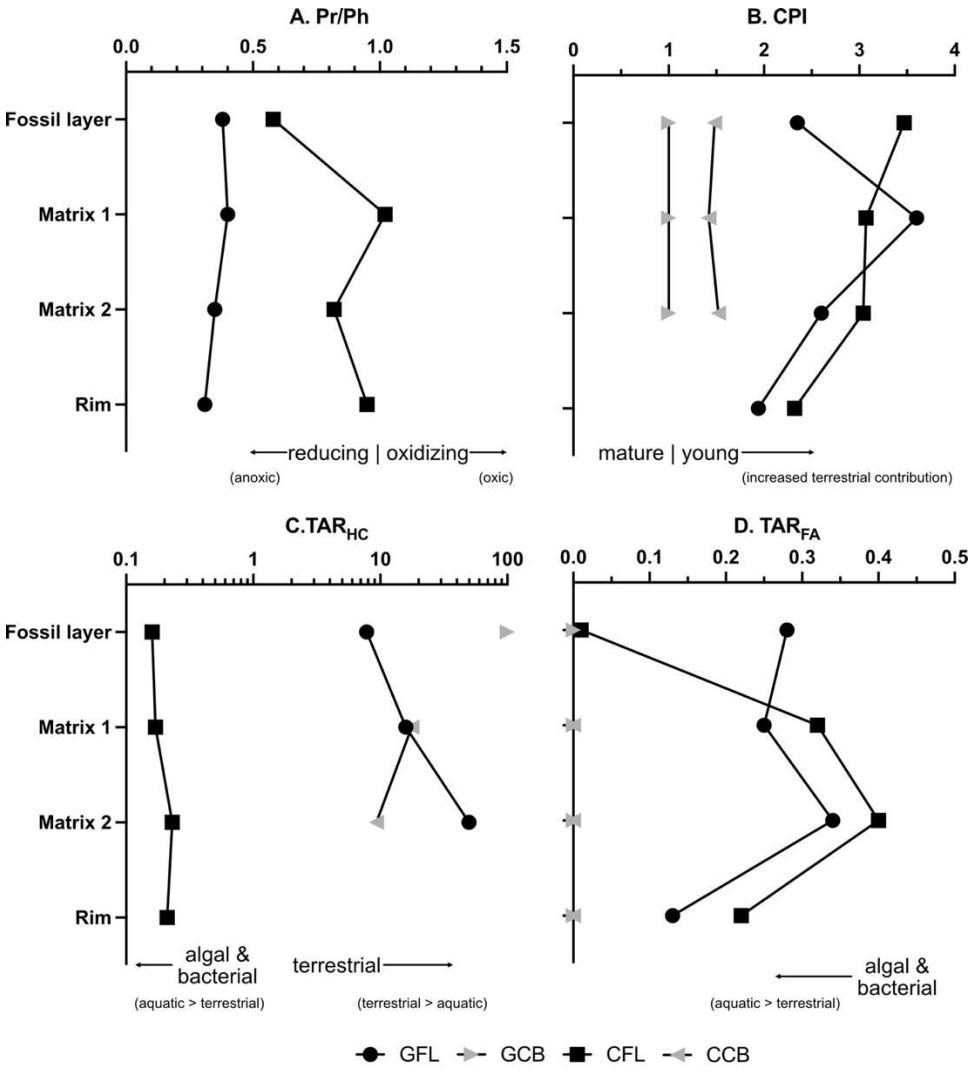

Figure 5: Fatty acids (F2). Freely extractable fatty acids from Greenland and Canada were abundant and diverse in structure. (a) Greenland free lipids display an even-carbon preference for long-chain ($C_{20:0}$ – $C_{30:0}$) fatty acids with a C_{max} at $C_{24:0}$ while carbonate-bound lipids (right y-axis) also display an even-carbon preference but with a C_{max} at $C_{20:0}$. $C_{16:0}$ and $C_{18:0}$ exceeded the y-axis window selected here and are therefore shown in the small box. (b) Canada free lipids

This article is protected by copyright. All rights reserved

display an even-carbon preference for long-chain ($C_{20:0}$ – $C_{30:0}$) fatty acids with a C_{max} at $C_{24:0}$. Carbonate-bond lipids (right y-axis) could only be detected via extracted ion chromatogram (EIC) of m/z 74 and reveal mostly non-specific short-chain fatty acids ($C_{14:0}$ – $C_{18:0}$).

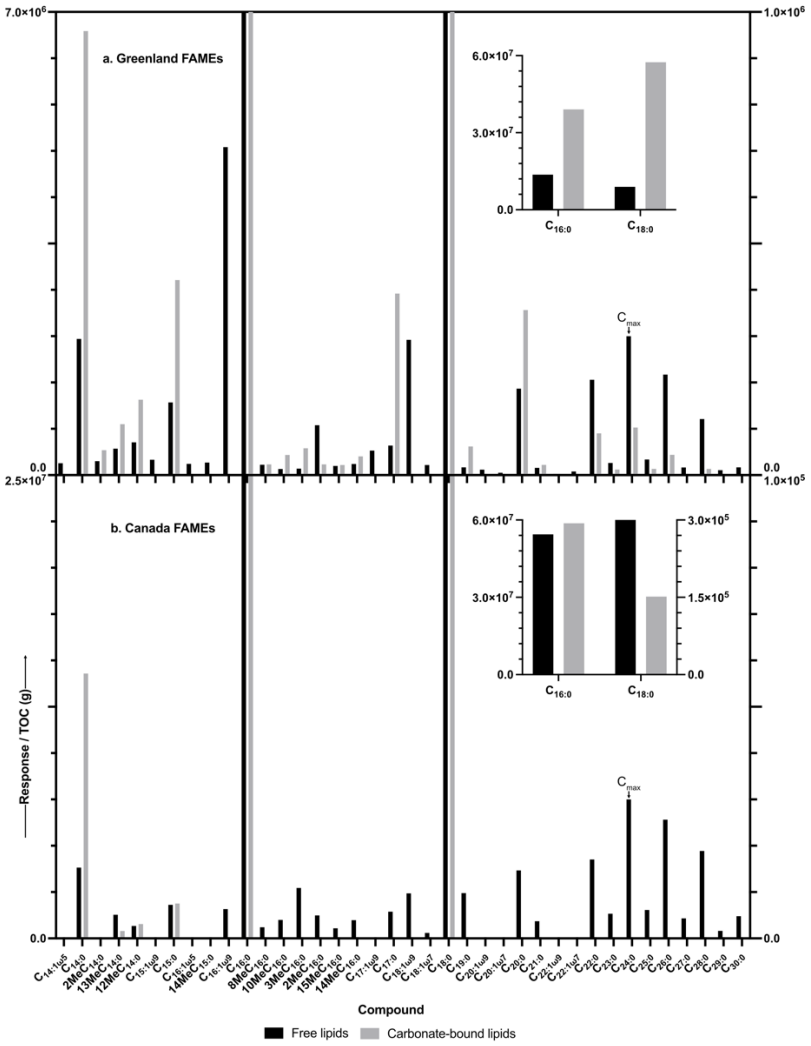

This article is protected by copyright. All rights reserved

Figure 6: Principal component analysis. Fatty acids found across all samples and in modern capelin were designated as variables and their values are represented by the integrated area (response/TOC (g)) in the F2 total ion chromatogram (TIC). (a) PC1 vs PC2. (b) PC1 vs PC3. Blue circles do no indicate statistical significance; however, they are used to identify compounds which are too tightly grouped to discretely label. (a) CFL samples are most influenced by bacterial and environmental lipids in PC1, (b) GFL samples are most influenced by algal lipids in PC2, (c) GFL samples are influenced by a mixture of algal lipids and capelin soft-tissue in PC3, and CFL0 groups with carbonate fractions.

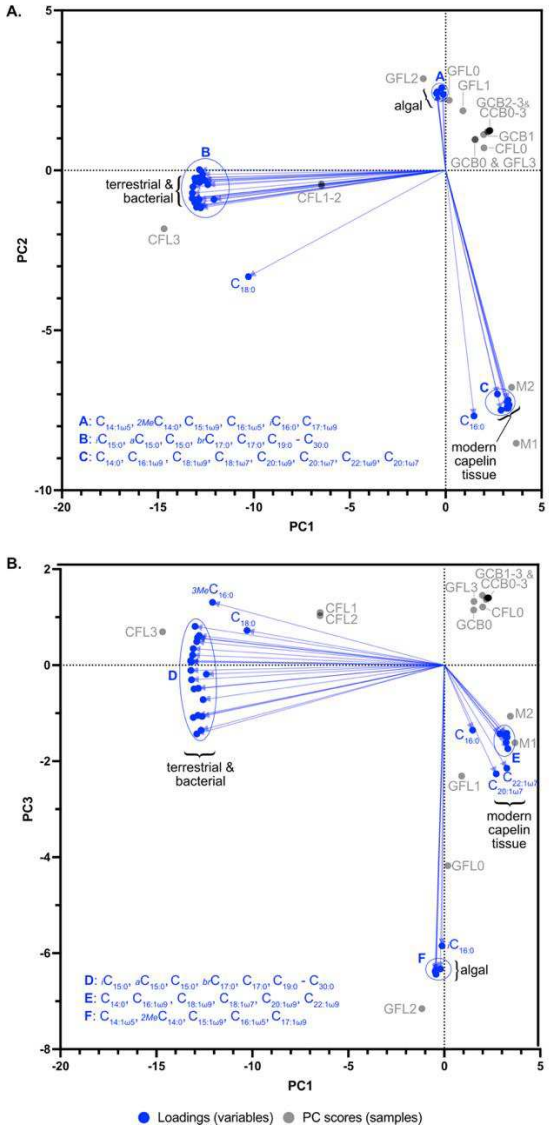

This article is protected by copyright. All rights reserved

Figure 7: Saturated hydrocarbon fraction $\delta^{13}C$ data (F1). Isotope measurements from both Kangerlussuaq and Ottawa varied from -29 ‰ to -32 ‰ without defined structure.

Canada free n = 6, Greenland free n = 9, Greenland carbonate-bound n = 6.

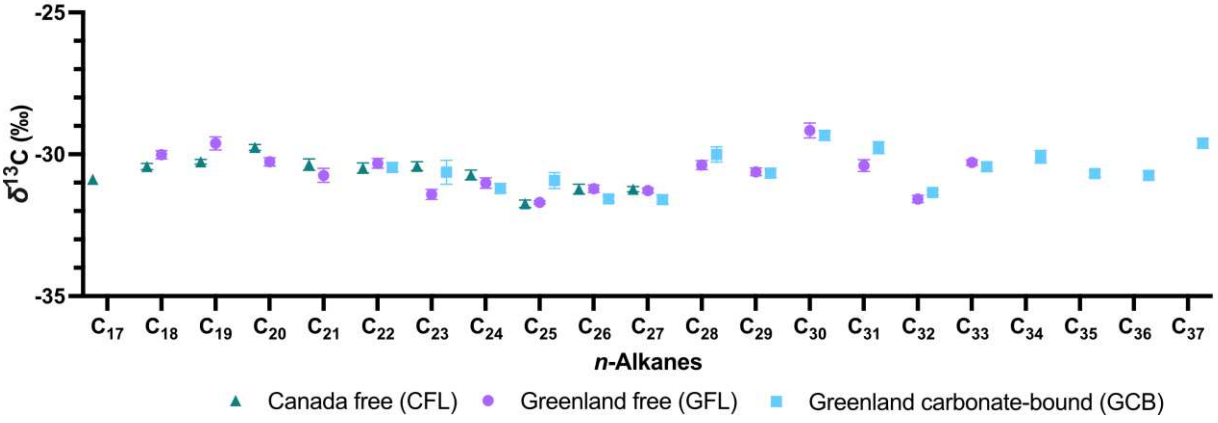

Figure 8: Major fatty acid $\delta^{13}C$ data. Short-chain ($C_{14:0}$ – $C_{18:0}$) isotope measurements varied from -24‰ to -30. Long-chain ($C_{19:0}$ – $C_{30:0}$) measurements spanned a narrower range -28 to -32‰.

Modern n = 3, Canada free n=6, Canada carbonate-bound = 6, Greenland free n = 9, Greenland carbonate-bound n = 6.

This article is protected by copyright. All rights reserved

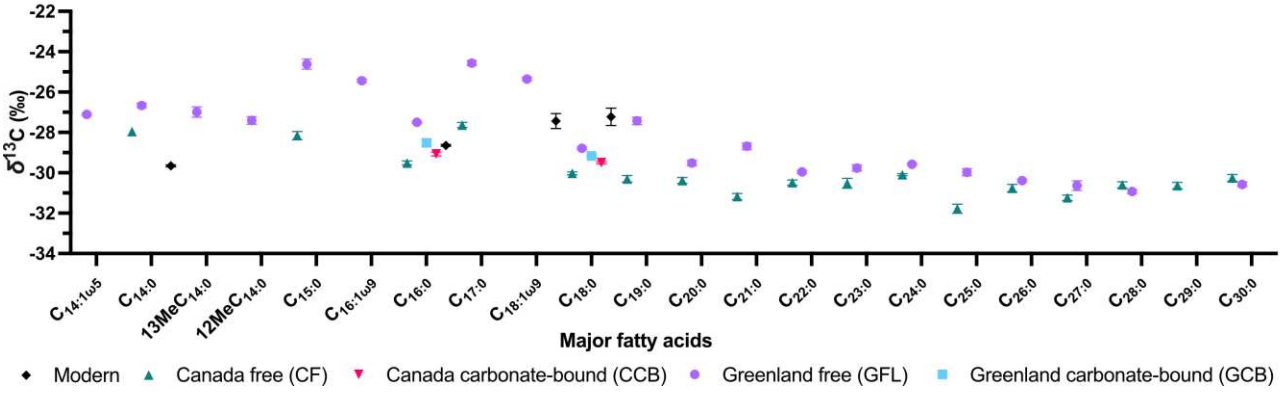

Table 1: Environment summary, ages, and composition across all samples.

	Greenland				Canada			
Summary								
Environment	marine				brackish-fresh[1]			
Estimated age (yrs)	6,000 - 7,000[2]				10,000 - 11,000[3]			
Composition								
	fossil[*]	*matrix 1*	*matrix 2*	*rim*	*fossil*	*matrix 1*[+]	*matrix 2*	*rim*

This article is protected by copyright. All rights reserved

TOC (%)	5.50	5.15	5.30	5.10	5.51	5.62	5.54	5.64
Carbonate (%)	57	58	56	57	55	55	56	55

[1]Desaulniers and Cherry, 1989, [2]Brink, 1975, [3]Gadd, 1980

This article is protected by copyright. All rights reserved

Table 2: Compound identification, abbreviations, and sample detection.

Compound	Abbreviation(s)	Modern	Greenland		Canada	
			free	*carbonate*	*free*	*carbonate*
n-Alkyl compounds						
n-alkanes	C_{16} … C_{38}	-	+	+	+	+
branched-chain alkanes	$^{br}C_{17}$ … $^{br}C_{20}$	-	+	-	+	-
n-alkanols	$C_{12\text{-}1}$ … $C_{32\text{-}1}$	-	+	+	+	-
alkan-2-ols	$C_{21\text{-}2}$ … $C_{25\text{-}2}$	-	+	+	-	-
methyl *n*-ketones	C_{19} … C_{33}	-	-	-	+	-
Fatty Acids						
Straight-chain saturated fatty acids (< 20 carbons)	$C_{14:0}$ … $C_{19:0}$	+	+	+	+	+
Long-straight-chain saturated fatty acids	$C_{20:0}$ … $C_{30:0}$	-	+	+	+	-
12-methyl tridecanoic acid ($C_{14:0}$ iso)	$^{12Me}C_{13:0}$	-	+	+	-	-
tetradec-9-enoic acid	$C_{14:1\omega5}$	-	+	-	-	-
2-methyl tetradecanoic acid	$^{2Me}C_{14:0}$	-	+	+	-	-
13-methyl tetradecanoic acid ($C_{15:0}$ iso)	$^{13Me}C_{14:0}$	-	+	+	+	+
12-methyl tetradecanoic acid ($C_{15:0}$ anteiso)	$^{12Me}C_{14:0}$	-	+	+	+	+
pentadec-6-enoic acid	$C_{15:1\omega9}$	-	+	-	-	-
hexadec-11-enoic acid	$C_{16:1\omega5}$	-	+	-	-	-

This article is protected by copyright. All rights reserved

14-methyl pentadecanoic acid ($C_{16:0}$ iso)	$^{14Me}C_{15:0}$	-	+	-	-	-
hexadec-9-enoic acid	$C_{16:1\omega7}$	+	-	-	-	-
hexadec-7-enoic acid	$C_{16:1\omega9}$	-	+	-	+	-
3-methyl hexadecanoic acid	$^{3Me}C_{16:0}$	-	+	+	+	-
8-methyl hexadecanoic acid	$^{8Me}C_{16:0}$	-	+	+	+	-
10-methyl hexadecanoic acid	$^{10Me}C_{16:0}$	-	+	+	+	-
2-methyl hexadecanoic acid	$^{2Me}C_{16:0}$	-	+	+	+	-
15-methyl hexadecanoic acid ($C_{17:0}$ iso)	$^{15Me}C_{16:0}$	-	+	+	+	-
14-methyl hexadecanoic acid ($C_{17:0}$ anteiso)	$^{14Me}C_{16:0}$	-	+	+	+	-
heptadec-10-enoic acid	$C_{17:1\omega9}$	-	+	-	-	-
octadeca-9,12-dienoic acid	$C_{18:2\omega6}$	+	+	-	-	-
octadec-9-enoic acid	$C_{18:1\omega9}$	+	+	-	+	-
octadec-11-enoic acid	$C_{18:1\omega7}$	+	+	-	+	-
icos-11-enoic acid	$C_{20:1\omega9}$	+	+	-	-	-
docos-11-enoic acid	$C_{22:1\omega11}$	+	+	-	-	-
docos-13-enoic acid	$C_{22:1\omega9}$	+	+	-	-	-
α-hydroxy fatty acids	$\alpha C_{22:0}$ ... $\alpha C_{30:0}$	-	+	+	-	-
β-hydroxy fatty acids	$\beta C_{14:0}$ ... $\beta C_{18:0}$	-	+	+	-	-
$C_{15:0}$ methyl-branched β-hydroxy fatty acids	$a\beta C_{15:0}$, $i\beta C_{15:0}$	-	+	+	-	-
ω-hydroxy fatty acids	$\omega C_{16:0,}$ $\omega C_{22:0,}$	-	+	+	-	-
dicarboxylic fatty acids	α,ω-fa	-	-	+	-	+

This article is protected by copyright. All rights reserved

Steroids						
5β-cholestan-3β-ol (coprostanol)	$C_{27}^{5\beta,3\beta}$	-	+	+	-	-
5β-cholestan-3α-ol (epicoprostanol)	$C_{27}^{5\beta,3\alpha}$	-	+	-	-	-
cholest-5-en-3β-ol (cholesterol)	$C_{27}\triangle^{5}$	+	+	+	+	-
5α-cholestan-3β-ol (cholestanol)	$C_{27}^{5\alpha,\ 3\beta}$	-	+	+	-	-
24-methyl-cholest-5-en-3β-ol (campesterol)	$C_{28}\triangle^{5,22}$	-	+	-	-	-
24β-ethyl-5β-cholestan-3β-ol (5β-stigmastanol)	$C_{29}^{24\beta,5\beta,3\beta}$	-	+	+	-	-
24β-ethyl-5β-cholestan-3α-ol (epi-5β-stigmastanol)	$C_{29}^{24\beta,5\beta,3\alpha}$	-	+	+	-	-
24-ethyl-cholest-5,22-dien-3β-ol (stigmasterol)	$C_{29}\triangle^{5,22}$	-	+	+	-	-
24-ethyl-cholest-5-en-3β-ol (β-sitosterol)	$C_{29}\triangle^{5}$	-	+	+	-	-
24α-ethyl-5α-cholestan-3β-ol (5α-stigmastanol)	$C_{29}^{24\beta,5\alpha,3\beta}$	-	+	+	-	-
Hopanoids						
17β,21β(H)-hopan-30-ol	$\beta\beta C_{30}$	-	+	-	+	-
17β,21β(H)-hopan-31-ol	$\beta\beta C_{31}$	-	+	-	+	-
17β,21β(H)-bishomohopan-32-ol	$\beta\beta C_{32}$	-	+	+	-	-
Terpenoids						
3α-hydroxy-5β-cholanic acid (lithocholic acid)	LCA	-	-	+	-	-
β-amyrin	β-am	-	+	+	-	-

This article is protected by copyright. All rights reserved

α-amyrin	α-am	-	+	+	-	-
11-oxo-α-amyrin	oxo-α-am	-	+	-	-	-
Miscellaneous						
norpristane	npr	-	-	-	+	-
pristane	pr	-	+	-	+	-
phytane	ph	-	+	-	+	-
phytol	phy	-	+	+	-	-
pyrene	py	-	+	-	+	-
retene	re	-	-	-	+	-

This article is protected by copyright. All rights reserved

Table 1: Environment summary, ages, and composition across all samples.

	Greenland				Canada			
Summary								
Environment	marine				brackish-fresh[1]			
Estimated age (yrs)	6,000 - 7,000[2]				10,000 - 11,000[3]			
Composition								
	fossil[*]	*matrix 1*	*matrix 2*	*rim*	*fossil*	*matrix 1*[+]	*matrix 2*	*rim*
TOC (%)	5.50	5.15	5.30	5.10	5.51	5.62	5.54	5.64
Carbonate (%)	57	58	56	57	55	55	56	55

[1]Desaulniers and Cherry, 1989, [2]Brink, 1975, [3]Gadd, 1980

This article is protected by copyright. All rights reserved

Table 2: Compound identification, abbreviations, and sample detection.

Compound	Abbreviation(s)	Modern	Greenland		Canada	
			free	*carbonate*	*free*	*carbonate*
n-Alkyl compounds						
n-alkanes	C_{16} … C_{38}	-	+	+	+	+
branched-chain alkanes	$^{br}C_{17}$ … $^{br}C_{20}$	-	+	-	+	-
n-alkanols	$C_{12\text{-}1}$ … $C_{32\text{-}1}$	-	+	+	+	-
alkan-2-ols	$C_{21\text{-}2}$ … $C_{25\text{-}2}$	-	+	+	-	-
methyl *n*-ketones	C_{19} … C_{33}	-	-	-	+	-
Fatty Acids						
Straight-chain saturated fatty acids (< 20 carbons)	$C_{14:0}$ … $C_{19:0}$	+	+	+	+	+
Long-straight-chain saturated fatty acids	$C_{20:0}$ … $C_{30:0}$	-	+	+	+	-
12-methyl tridecanoic acid ($C_{14:0}$ iso)	$^{12Me}C_{13:0}$	-	+	+	-	-
tetradec-9-enoic acid	$C_{14:1\omega5}$	-	+	-	-	-
2-methyl tetradecanoic acid	$^{2Me}C_{14:0}$	-	+	+	-	-
13-methyl tetradecanoic acid ($C_{15:0}$ iso)	$^{13Me}C_{14:0}$	-	+	+	+	+
12-methyl tetradecanoic acid ($C_{15:0}$ anteiso)	$^{12Me}C_{14:0}$	-	+	+	+	+
pentadec-6-enoic acid	$C_{15:1\omega9}$	-	+	-	-	-
hexadec-11-enoic acid	$C_{16:1\omega5}$	-	+	-	-	-

This article is protected by copyright. All rights reserved

14-methyl pentadecanoic acid ($C_{16:0}$ iso)	$^{14Me}C_{15:0}$	-	+	-	-	-
hexadec-9-enoic acid	$C_{16:1\omega7}$	+	-	-	-	-
hexadec-7-enoic acid	$C_{16:1\omega9}$	-	+	-	+	-
3-methyl hexadecanoic acid	$^{3Me}C_{16:0}$	-	+	+	+	-
8-methyl hexadecanoic acid	$^{8Me}C_{16:0}$	-	+	+	+	-
10-methyl hexadecanoic acid	$^{10Me}C_{16:0}$	-	+	+	+	-
2-methyl hexadecanoic acid	$^{2Me}C_{16:0}$	-	+	+	+	-
15-methyl hexadecanoic acid ($C_{17:0}$ iso)	$^{15Me}C_{16:0}$	-	+	+	+	-
14-methyl hexadecanoic acid ($C_{17:0}$ anteiso)	$^{14Me}C_{16:0}$	-	+	+	+	-
heptadec-10-enoic acid	$C_{17:1\omega9}$	-	+	-	-	-
octadeca-9,12-dienoic acid	$C_{18:2\omega6}$	+	+	-	-	-
octadec-9-enoic acid	$C_{18:1\omega9}$	+	+	-	+	-
octadec-11-enoic acid	$C_{18:1\omega7}$	+	+	-	+	-
icos-11-enoic acid	$C_{20:1\omega9}$	+	+	-	-	-
docos-11-enoic acid	$C_{22:1\omega11}$	+	+	-	-	-
docos-13-enoic acid	$C_{22:1\omega9}$	+	+	-	-	-
α-hydroxy fatty acids	$\alpha C_{22:0}$ ... $\alpha C_{30:0}$	-	+	+	-	-
β-hydroxy fatty acids	$\beta C_{14:0}$ ... $\beta C_{18:0}$	-	+	+	-	-
$C_{15:0}$ methyl-branched β-hydroxy fatty acids	$a\beta C_{15:0}$, $i\beta C_{15:0}$	-	+	+	-	-
ω-hydroxy fatty acids	$\omega C_{16:0,}$ $\omega C_{22:0,}$	-	+	+	-	-
dicarboxylic fatty acids	α,ω-fa	-	-	+	-	+

This article is protected by copyright. All rights reserved

Steroids						
5β-cholestan-3β-ol (coprostanol)	$C_{27}^{5\beta,3\beta}$	-	+	+	-	-
5β-cholestan-3α-ol (epicoprostanol)	$C_{27}^{5\beta,3\alpha}$	-	+	-	-	-
cholest-5-en-3β-ol (cholesterol)	$C_{27}\triangle^{5}$	+	+	+	+	-
5α-cholestan-3β-ol (cholestanol)	$C_{27}^{5\alpha,\ 3\beta}$	-	+	+	-	-
24-methyl-cholest-5-en-3β-ol (campesterol)	$C_{28}\triangle^{5,22}$	-	+	-	-	-
24β-ethyl-5β-cholestan-3β-ol (5β-stigmastanol)	$C_{29}^{24\beta,5\beta,3\beta}$	-	+	+	-	-
24β-ethyl-5β-cholestan-3α-ol (epi-5β-stigmastanol)	$C_{29}^{24\beta,5\beta,3\alpha}$	-	+	+	-	-
24-ethyl-cholest-5,22-dien-3β-ol (stigmasterol)	$C_{29}\triangle^{5,22}$	-	+	+	-	-
24-ethyl-cholest-5-en-3β-ol (β-sitosterol)	$C_{29}\triangle^{5}$	-	+	+	-	-
24α-ethyl-5α-cholestan-3β-ol (5α-stigmastanol)	$C_{29}^{24\beta,5\alpha,3\beta}$	-	+	+	-	-
Hopanoids						
17β,21β(H)-hopan-30-ol	$\beta\beta C_{30}$	-	+	-	+	-
17β,21β(H)-hopan-31-ol	$\beta\beta C_{31}$	-	+	-	+	-
17β,21β(H)-bishomohopan-32-ol	$\beta\beta C_{32}$	-	+	+	-	-
Terpenoids						
3α-hydroxy-5β-cholanic acid (lithocholic acid)	LCA	-	-	+	-	-
β-amyrin	β-am	-	+	+	-	-

This article is protected by copyright. All rights reserved

α-amyrin	α-am	-	+	+	-	-
11-oxo-α-amyrin	oxo-α-am	-	+	-	-	-
Miscellaneous						
norpristane	npr	-	-	-	+	-
pristane	pr	-	+	-	+	-
phytane	ph	-	+	-	+	-
phytol	phy	-	+	+	-	-
pyrene	py	-	+	-	+	-
retene	re	-	-	-	+	-

This article is protected by copyright. All rights reserved

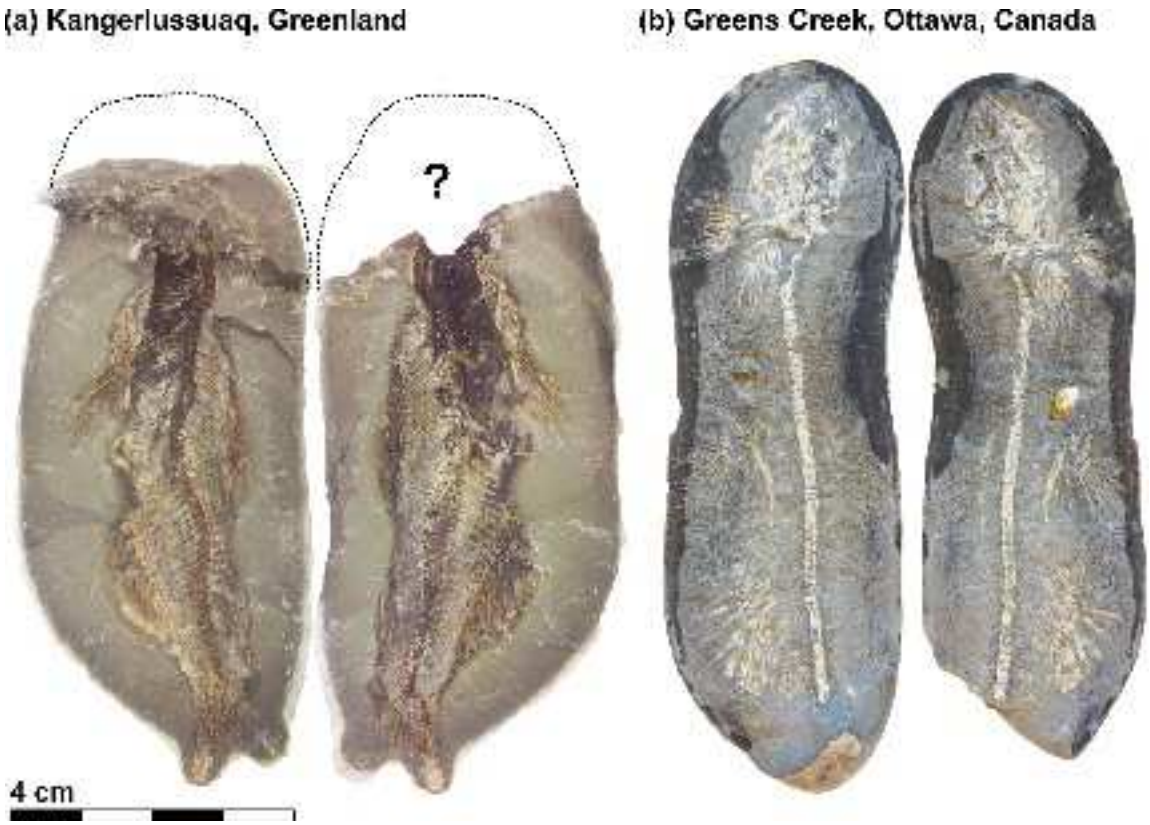

gbi_12480_f1.png

This article is protected by copyright. All rights reserved

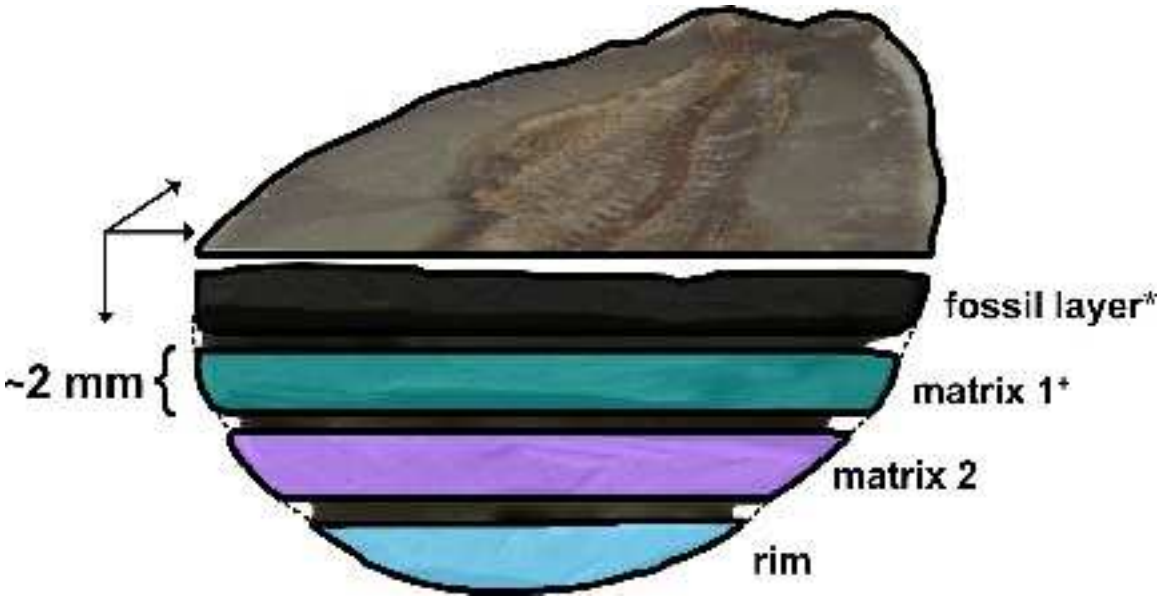

gbi_12480_f2.png

This article is protected by copyright. All rights reserved

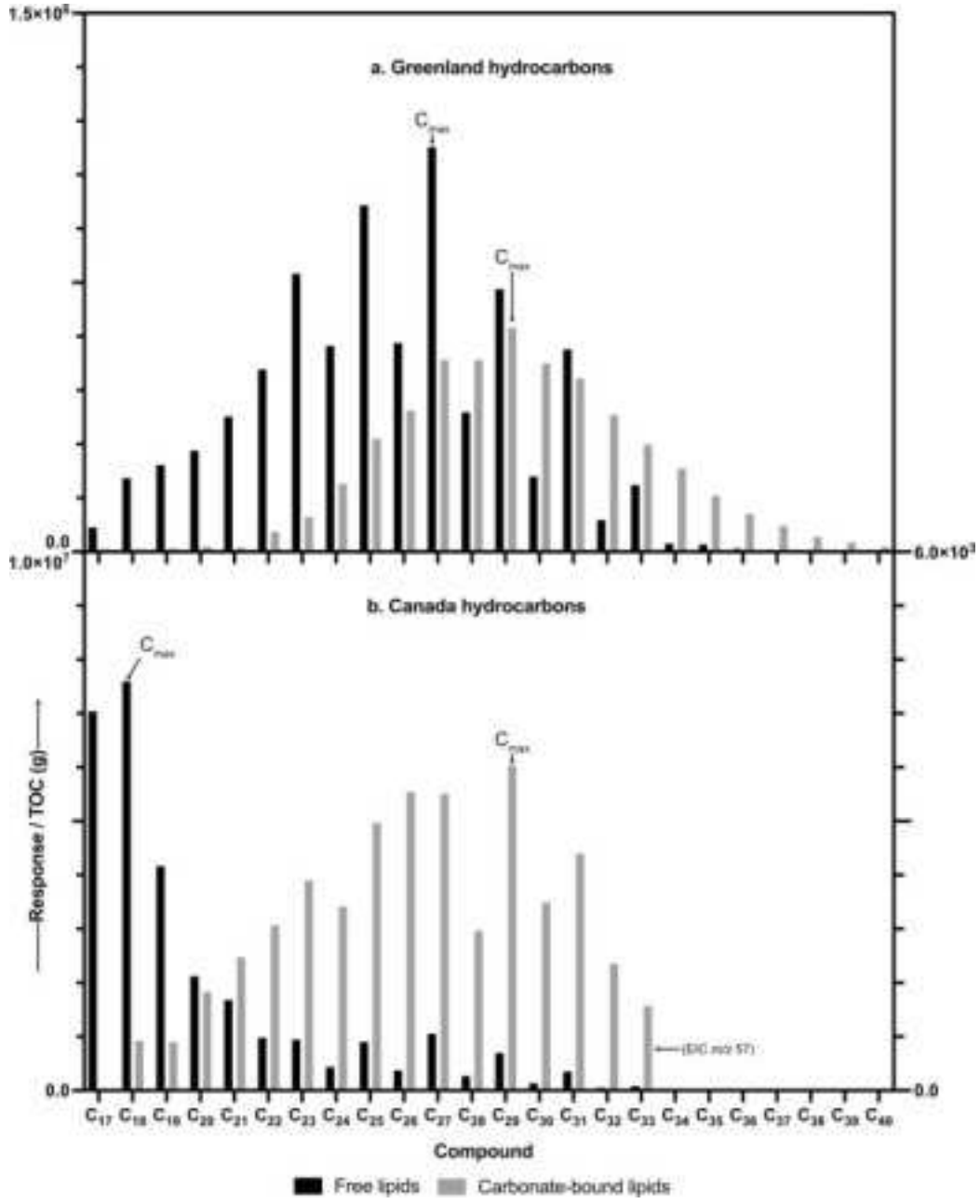

gbi_12480_f3.png

This article is protected by copyright. All rights reserved

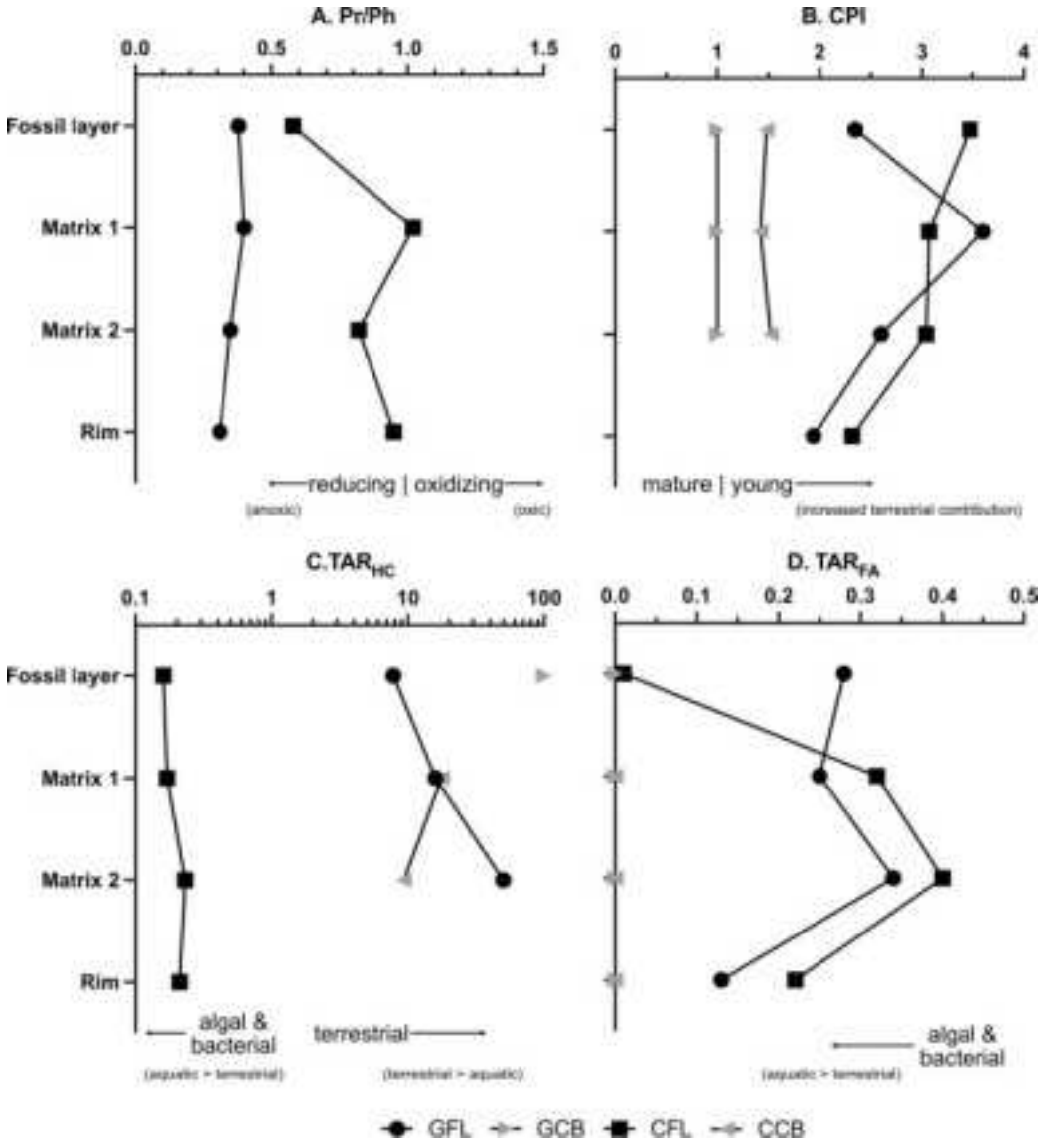

gbi_12480_f4.png

This article is protected by copyright. All rights reserved

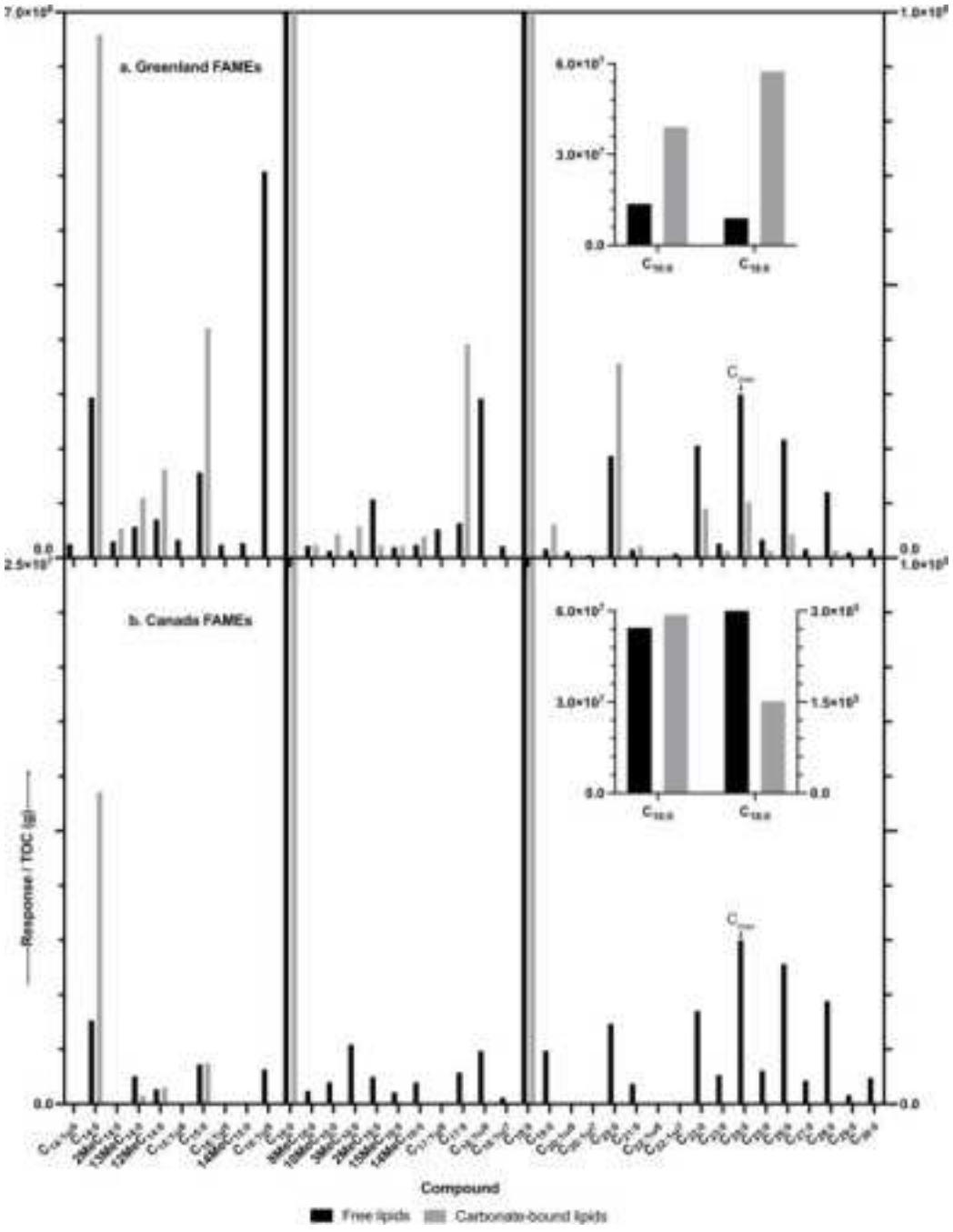

gbi_12480_f5.png

This article is protected by copyright. All rights reserved

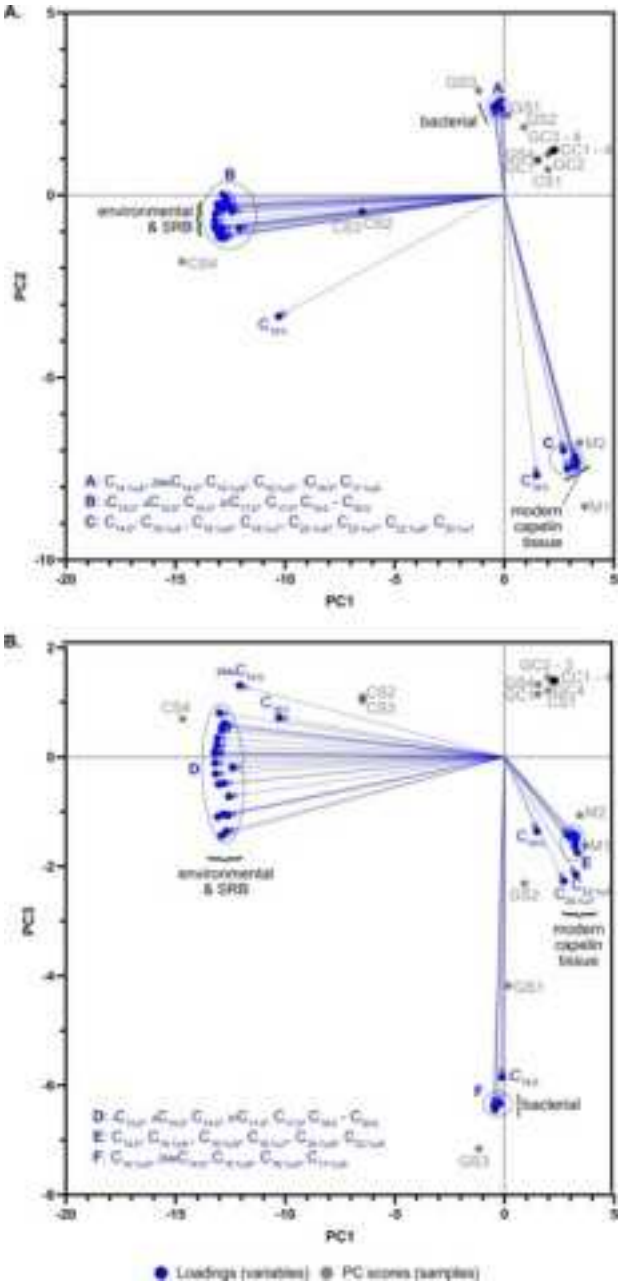

gbi_12480_f6.png

This article is protected by copyright. All rights reserved

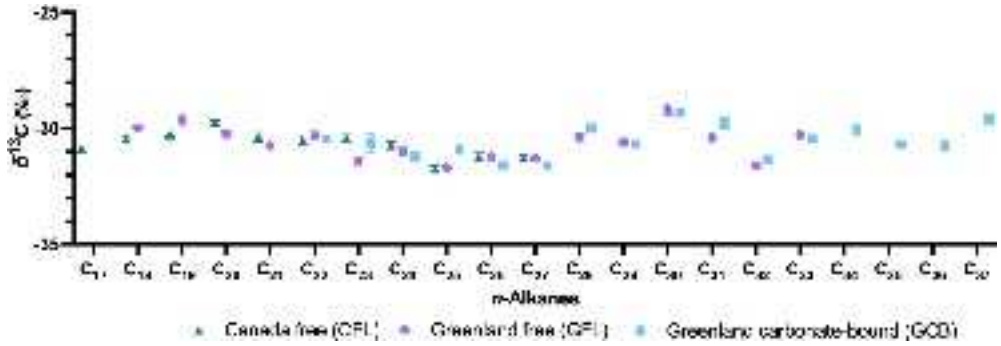

gbi_12480_f7.png

This article is protected by copyright. All rights reserved

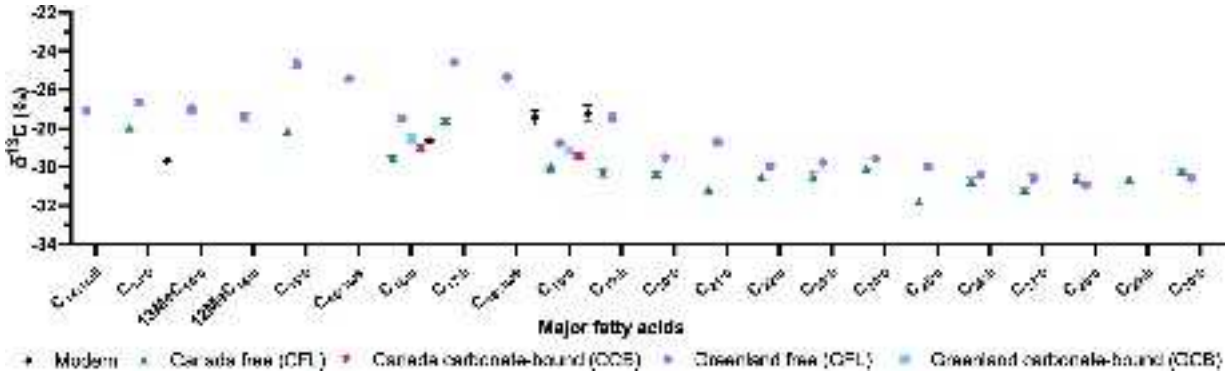

gbi_12480_f8.png

This article is protected by copyright. All rights reserved